universität wien

DIPLOMARBEIT / DIPLOMA THESIS

Titel der Diplomarbeit / Title of the Diploma Thesis

„Isolation and characterization of bioactive constituents from *Pterocarpus santalinus* affecting the healthspan of *Caenorhabditis elegans*“

verfasst von / submitted by

Karina Ptak

angestrebter akademischer Grad / in partial fulfilment of the requirements for the degree of

Magistra der Pharmazie (Mag.pharm.)

Wien, 2021 / Vienna, 2021

Studienkennzahl lt. Studienblatt / degree programme code as it appears on the student record sheet:	A 449
Studienrichtung lt. Studienblatt / degree programme as it appears on the student record sheet:	Diplomstudium Pharmazie
Betreut von / Supervisor:	Univ.-Prof. Dr. Judith M. Rollinger

ACKNOWLEDGEMENT

First and foremost, I would like to thank Univ.-Prof. Mag. pharm. Dr. Judith M. Rollinger for giving me the opportunity to perform my diploma thesis in the Department of Pharmacognosy. For me, her charismatic enthusiasm and passion for research and the world of plants, as well as her caring and motivating personality are very inspiring and have very much sparked my curiosity for the world of pharmacognosy.

Especially, I would like to express my deep appreciation and gratitude to my supervisor Mag. Julia Zwirchmayr for the motivation, patience as well as the immeasurable help and excellent support during the entire process of my diploma thesis. You were the best supervisor anyone could wish for, thank you for letting me learn from you and for all the fun we had.

I also gratefully acknowledge ao. Univ.-Prof. Mag. Dr. Ernst Urban for the NMR measurements.

Additionally, I would like to thank the whole team of the Pharmacognosy Department for all the support and the great working atmosphere. Many thanks also to Franziska Höller BSc. for introducing me to the opportunity of being part of this great team.

I am very grateful for my friends Roland and Tom; it was a real pleasure to work with you in the Department at the same time. I am especially grateful for our clique, full of great people I met throughout my studies and now am honored to call my friends.

I want to say *Thank you* to my family and friends, especially my parents and sister for all the love, support and encouragement throughout the years. Last but not least, my deepest gratitude to the love of my life, Constantin. From beginning to end, you have been the biggest support for me on this journey – thank you so much!

TABLE OF CONTENTS

LIST OF ABBREVIATIONS

AA	Acetic acid
ATPase	Adenyl pyrophosphatase
$CHCl_3$	Chloroform
CCl4	Tetrachloromethane
C. elegans	*Caenorhabditis elegans*
DCM	Dichloromethane
DMSO	Dimethylsulfoxid
DPPH	2,2-diphenyl-1-picrylhydrazyl
DT_{50}	Dead Time 50 (Timepoint, when 50% of worms were dead)
EGCG	Epigallocatechin gallate
EtOAc	Ethyl acetate
FA	Formic acid
FOXO3	Forkhead Box O3
H_2O	Water
H_2SO_4	Sulfuric acid
HEMWat	*n*-Hexane, Ethyl acetate, Methanol, Water
HPCCC	High-Performance Counter-Current Chromatography
IC_{50}	half maximal inhibitory concentration
IIS	Insulin/IGF-1 signaling
MeOH	Methanol
n-hex	Hexan
PDA	Photo Diode Array
PE	Petroleum ether
P. santalinus	*Pterocarpus santalinus*
SSo	Stock solution
TLC	Thin Layer Chromatography
TNF α	Tumor Necrosis Factor alpha
UHPLC	Ultra High-Performance Liquid Chromatography
UV	Ultraviolet

1 ABSTRACT

Since the beginning of time, understanding the aging process has been a central question in human history. The nematode *Caenorhabditis elegans* (*C. elegans*) has been one of the most important model organisms in aging research for decades. This diploma thesis is dedicated to *Pterocarpus santalinus* L.f., commonly known as red sandalwood. Its methanol-dichloromethane generated heartwood extract showed promising lifespan prolonging effects on the nematodes on the one hand and is still insufficiently phytochemically studied on the other hand. The following work can be thematically divided into two sections: (i) Isolation and Characterization of bioactive constituents from *P. santalinus* affecting the healthspan of *C. elegans* and (ii) the phenotypic screening of selected samples affecting the healthspan of *C. elegans.*

In a previous study, a large-scale extraction of *P. santalinus* heartwood (PtesanXDM) was performed and 13 fractions (PS01_01 - PS01_13) were subsequently generated by High-Performance Counter-Current Chromatography (HPCCC), which showed significant activity on the nematode lifespan in a *C. elegans* lifespan assay. Two of these HPCCC fractions, namely PS01_04 and PS01_07 were further separated by sephadex column chromatography (CC) during the course of this work and two isolates were identified as pterostilbene (PS-A) and santal (PS-B) by 1D- and 2D-NMR structural elucidation. Both compounds have previously been described for *P. santalinus*.

To facilitate the isolation and characterization of additional bioactive constituents, the next step was to separate a large amount of the polar, highly staining pigments of the crude extract PtesanXDM by liquid-liquid chromatography. The obtained fraction PtesanXDM_DCM, enriched with secondary metabolites was able to prolong the lifespan of the worms whereas the pigment-enriched fraction PtesanXDM_MW showed no effects in the *C. elegans* lifespan assay. PtesanXDM_DCM was further separated into 4 sub-fractions (i.e. PSD01_01 - PSD01_04) via Puriflash Interchim. Each fraction obtained from the phytochemical workup was again tested in the *C. elegans* lifespan assay. At a concentration of 10 µg/mL, fraction PSD01_01 resulted in a DT_{50} prolongation (= death-time 50%; DT_{50}) of 19.4% (although not significant); interestingly, at 25 µg/mL, fraction PSD01_02 significantly decreased the DT_{50} value by 31.6%. At the lower concentration of 10 µg/mL, this life-shortening effect disappeared. Fraction PSD01_03 represented the most active and complex fraction. Similarily than the positive control reserpine, this

fraction prolonged the mean survival of nematodes by 36.9% and 36.2% (at 25 and 10 µg/mL, respectively; $p < 0.05$ in each case) compared to the untreated control. The study of fraction PSD01_03 will be the subject of further work at the Division of Pharmacognosy. The pigment-enriched fraction PSD01_04 showed little effect on *C. elegans* lifespan.

Within the scope of this diploma thesis, fraction PSD01_01 and PSD01_02 were further fractionated via hyphenation of the Puriflash Interchim with the HPCCC. PSD01_01 was separated into tree sub-fractions (i.e. PSD02_01 - PSD02_03), whereas PSD01_02 into eight sub-fractions (i.e PSD03_01 - PSD03_08). All sub-fractions were assayed for lifespan prolongation in the *C. elegans* lifespan assay. PSD02_01 - PSD02_03 were able to increase the DT_{50} value of nematodes by 20.9% ($p < 0.05$), 16.2% (n.s.) and 24.5% ($p < 0.01$), respectively. Further, PSD03_01, PSD03_03 and PSD03_04 significantly resulted in DT_{50} prolongation of 19.8% ($p < 0.05$), 31.7% ($p < 0.01$) and 25.1% ($p < 0.01$), respectively. On the contrary, PSD03_05 showed detrimental effects on the mean survival rate of nematodes with a DT_{50} reduction of 28.2% ($p < 0.01$).

In the second part of the present thesis, previously generated HPCCC fractions of the crude extract PtesanXDM, namely PS01_01 - PS01_13, were examined in different *C. elegans* assays on wild-type worms (N2), *daf-16* loss-of-function (CF1038) and *skn-1* loss-of-function (EU1) mutants. In a lifespan assay with the wild-type worms (N2), fractions PS01_01, PS01_05, PS01_08 and PS01_13 resulted in a significant DT_{50} increase of 25.1% ($p < 0.01$), 17.6% ($p < 0.05$), 16.7% ($p < 0.05$) and 19.0% ($p < 0.05$), respectively. On the contrary, PS01_04, caused a significant decrease of the mean survival rate by 33.5% ($p < 0.01$) when compared to the vehicle control. The lifespan-prolonging/shortening effect of these fractions could not be detected in a lifespan assay using the *daf-16* loss-of-function mutants, suggesting that all fractions, with the exception of fraction PS01_04, are dependent on the presence of the transcription factor *daf-16*. Further, a juglone-induced stress resistance assay was performed with both, wild-type worms and *daf-16* loss-of-function mutants. Again, it was shown that the stress resistance of wild-type worms is dependent on the presence of *daf-16*. In turn, the stress resistance assay with *skn-1* loss-of-function mutants could confirm the lifespan prolonging effect by PtesanXDM, suggesting that the lifespan prolonging effect of the wild-type worms is not dependent on *skn-1*.

ABSTRACT (DEUTSCH)

Seit Anbeginn der Zeit ist es eine zentrale Frage der Menschheitsgeschichte, den Alterungsprozess zu verstehen. Der Fadenwurm *Caenorhabditis elegans* (*C. elegans*) stellt seit Jahrzehnten einen der wichtigsten Modellorganismen für die Altersforschung dar. Diese Diplomarbeit widmet sich *Pterocarpus santalinus* L.f., allgemein auch bekannt als Rotes Sandelholz. Der durch Methanol-Dichlormethan gewonnene Kernholzextrakt zeigt einerseits eine vielversprechende lebensverlängernde Wirkung auf Nematoden, und ist andererseits noch unzureichend phytochemsich untersucht. Die folgende Arbeit lässt sich thematisch in zwei Abschnitte gliedern: (i) Isolierung und Charakterisierung von *C. elegans* lebensverlängernden Bestandteilen aus *P. santalinus* und (ii) dem phänotypischen Screening ausgewählter Proben, welche die Lebensspanne der Nematoden positiv beeinflussen.

In einer vorausgehenden Studie wurde das Kernholz mittels Extraktion mit Methanol und Dichlormethan im Großmaßstab durchgeführt (i.e. PtesanXDM). Aus dem gewonnenen Rohextrakt wurden anschließend durch Hochleistungs-Gegenstromchromatographie (HPCCC) 13 Fraktionen generiert (PS01_01 – PS01_13), die in einem *C. elegans* Lifespan-Assay eine signifikante Aktivität auf die Lebensspanne der Nematoden zeigten. Zwei dieser HPCCC Fraktionen (PS01_04 uns PS01_07) wurden im Laufe dieser Arbeit durch Sephadex-Säulenchromatographie aufgetrennt und zwei daraus gewonnene Isolate mittels 1D- und 2D-NMR-Strukturaufklärung als Pterostilbene (PS-A) und Santal (PS-B) identifiziert. Beide Verbindungen wurden bereits für *P. santalinus* beschrieben.

Um die Isolierung und Charakterisierung weiterer bioaktiver Inhaltsstoffe zu ermöglichen, wurde im nächsten Schritt eine große Menge der polaren, stark färbenden Pigmente des Rohextraktes PtesanXDM durch Flüssig-Flüssig-Chromatographie mittels eines Scheidetrichters abgetrennt. Die gewonnene, mit Sekundärmetaboliten angereicherte bzw. Pigment-abgereicherte Fraktion (PtesanXDM_DCM), die die Lebensspanne der Würmer verlängerte, wurde phytochemsich untersucht und mittels Puriflash Interchim in die Fraktionen PSD01_01 – PSD01_04 weiter aufgetrennt. Jede Fraktion, die während der phytochemischen Aufarbeitung aus PtesanXDM gewonnen wurde, wurde im *C. elegans* Lifespan-Assay ausgetestet. Die Fraktion PSD01_01 führte bei einer Konzentration von 10 µg/mL zu einer nicht signifikanten DT_{50}-Verlängerung (= death-time 50%; DT_{50}) von 19.4%; die Fraktion PSD01_02 verringerte interessanterweise bei 25 µg/mL den DT_{50}-Wert signifikant um 31.6%. Bei der niedrigeren Konzentration von 10 µg/mL war dieser lebenszeitverkürzende Effekt aufgehoben. Die Fraktion PSD01_03 stellte die aktivste und

komplexeste Fraktion dar und verlängerte - vergleichbar mit der Positivkontrolle Reserpin - die mittlere Überlebensrate der Nematoden um 36.9% (25 µg/mL) und 36.2% (10 µg/mL; jeweils $p < 0.05$) im Vergleich zur unbehandelten Kontrolle. Die Untersuchung der Fraktion PSD01_03 wird Gegenstand weiterer Arbeiten am Department sein. Die mit Pigmenten angereicherte Fraktion PSD01_04 zeigte kaum Auswirkungen auf die Lebensspanne von *C. elegans.* Im Rahmen dieser Diplomarbeit wurden die Fraktionen PSD01_01 und PSD01_02 über eine Kopplung der Puriflash Interchim mit der HPCCC weiter fraktioniert. Die Fraktion PSD01_01 wurde weiter in drei Fraktionen PSD02_01 – PSD02_03 und die Fraktion PSD01_02 in acht Fraktionen PSD03_01 – PSD03_08 aufgetrennt. Alle Unterfraktionen wurden im *C. elegans*-Lifespan-Assay auf einen möglichen lebensverlängernden Effekt untersucht. PSD02_01 - PSD02_03 konnten den DT_{50}-Wert der Nematoden um 20.9% ($p < 0.05$), 16.2% (n.s.) bzw. 24.5% ($p < 0.01$) erhöhen. Zudem führten PSD03_01, PSD03_03 und PSD03_04 signifikant zu einer DT_{50}-Verlängerung von 19.8% ($p < 0.05$), 31.7% ($p < 0.01$) bzw. 25.1% ($p < 0.01$). PSD03_05 zeigte signifikant verkürzende Effekte auf die mittlere Überlebensrate der Nematoden mit einer DT_{50}-Reduktion von 28.2% ($p < 0.01$).

Im zweiten Teil dieser Arbeit wurden die zuvor generierten HPCCC Fraktionen PS01_01 – PS01_13 des Rohextraktes PtesanXDM in unterschiedlichen *C. elegans* Assays an Wildtyp Würmern (N2), *daf-16* loss-of-function (CF1038) und *skn-1* loss-of-function (EU1) Würmern untersucht. In einem Lifespan-Assay mit den Wildtyp-Würmern (N2) führten die Fraktionen PS01_01, PS01_05, PS01_08 und PS01_13 zu einer signifikanten DT_{50}-Erhöhung von 25.1% ($p < 0.01$), 17.6% ($p < 0.05$), 16.7% ($p < 0.05$) und 19. 0% ($p < 0.05$). Im Gegensatz dazu verursachte PS01_04 eine signifikante Abnahme der mittleren Überlebensrate um 33.5% ($p < 0.01$) im Vergleich zur Vehikelkontrolle. Die lebensverlängernden/verkürzenden Effekte dieser Fraktionen konnten in einem Lifespan-Assay mit den *daf-16* Loss-of-Function-Mutanten nicht nachgewiesen werden, was darauf hindeutet, dass alle Fraktionen, mit Ausnahme der Fraktion PS01_04, von der Anwesenheit des Transkriptionsfaktors *Daf-16* abhängig sind. Des Weiteren wurde ein Juglon-induzierter Stressresistenz-Assay sowohl mit Wildtyp-Würmern als auch mit *daf-16* Loss-of-Function-Mutanten durchgeführt. Auch hier zeigte sich, dass die Stressresistenz der Wildtyp-Würmer von der Anwesenheit von *daf-16* abhängig ist. Im Gegenzug konnte der Stressresistenz-Assay mit *skn-1* loss-of-function Mutanten die lebensverlängernde Wirkung von PtesanXDM bestätigen, was darauf hindeutet, dass die lebensverlängernde Wirkung der Wildtyp-Würmer nicht von der Anwesenheit des Transkriptionsfaktors *skn-1* abhängig ist.

2 AIM OF THE WORK

2.1 Isolation and Characterization of Bioactive Constituents from *Pterocarpus santalinus* affecting the Health Span of *Caenorhabditis elegans*

The heartwood of *P. santalinus* is used as a traditional remedy with multiple uses. However, the constituents responsible for the manifold bioactivities reported so far are still unknown to a large extent. The aim of this thesis was to separate selected fractions of a lifespan prolonging extract generated from the heartwood of *P. santalinus* and to isolate and characterize putative bioactive constituents. The constituents to be isolated in this work were present in HPCCC fractions prepared from the heartwood extract PtesanXDM of a previous work. From two bioactive fractions, namely PS01_04 and PS01_07, the pure substances PS-A (pterostilbene) and PS-B (santal) were isolated. To facilitate further fractionation procedures by depletion of the highly staining pigments present in PtesanXDM, a liquid-liquid separation of the crude extract was performed. The resulting pigment-depleted fraction PtesanXDM_DCM was further separated via Interchim Puriflash in a large-scale manner. Four fractions, namely PSD01_01 - PSD01_04, were generated. PSD01_01 and PSD01_02 were further investigated by coupling the Interchim Puriflash with the HPCCC. PSD01_01 was fractionated into three sub-fractions (i.e. PSD02_01 - PSD02_03) and PSD01_02 was separated into eight sub-fractions (i.e. PSD03_01 - PSD03_08). Each fraction obtained during the phytochemical workup of PtesanXDM was tested and evaluated for its lifespan prolonging effects in the *C. elegans* lifespan assay on wild type worms (N2).

2.2 Phenotypic Screening of Selected Samples Affecting the Health Span of *Caenorhabditis elegans*

The aim of the second part of this thesis was to investigate selected fractions of PtesanXDM for their health span affecting properties in the nematode *C. elegans* using different worm strains. 13 HPCCC fractions were tested in a *C. elegans* lifespan assay on wild type worms (N2) and in a juglone-induced stress resistance assay with *daf-16* loss-of-function (CF1038) and *skn-1* loss-of-function (EU1) mutants, respectively. The aim of the juglone-induced stress resistance assays was to detect whether the lifespan prolonging effects of the 13 HPCCC fractions are dependent on the transcription factors *daf-16* and/or *skn-1*.

3 INTRODUCTION

3.1 Isolation and Characterization of Bioactive Constituents from *Pterocarpus santalinus* affecting the Health Span of *Caenorhabditis elegans*

3.1.1 Botanical Description of *Pterocarpus santalinus*

Pterocarpus santalinus L.f., also known as Red Sanders, belongs to the Fabaceae family and is an endemic plant species restricted to southern parts of the Eastern Ghats in India. Red Sanders is worldwide considered as endangered plant (Soundararajan, Ravi Kumar, Murugesan, & Chandrashekar, 2016). It is reported that the small to medium sized deciduous tree has also been introduced into other countries such as China, Pakistan, Sri Lanka and Taiwan (Figure 1). The bark of *P. santalinus* is blackish brown, the sapwood is white, and the heartwood is very hard and deep red to almost purplish black, which is mainly due to the santalins and santarubins, a series of strongly coloring pigments that range from purple to yellow (Figure 2). The main red dye, santalin A-C, accounts for 16% and is now used as a dye for textiles, medicine and food (Arunkumar & Joshi, 2014; Arunakumara, Walpola, Subasinghe, & Yoon, 2011). The leaves of *P. santalinus* are about 10-18 cm long and trifoliolate, the flowers are yellow, about 2 cm long and bisexual, and the flat legumes contain one or rarely two 1-1.5 cm long, reddish-brown seeds (Mohammad, Rajkapoor, & Kavimani, 2015).

Figure 1: *Pterocarpus santalinus* tree (https://commons.wikimedia.org/wiki/File:Red_sanders_tree,bramamgarimattam,A.P_-_panoramio.jpg; effective: May 2021)

Figure 2: *Pterocarpus santalinus* wood (https://propropertiesindia.com/wp-content/uploads/2021/03/SANDALWOOD.jpg; effective: May 2021)

3.1.2 Traditional and general use of *Pterocarpus santalinus*

P. santalinus is a very popular and valuable medicinal plant which is much in demand in domestic and international markets. Local physicians specialized in the Ayurvedic and Sidda systems of medicine have recognized the medicinal value of Red Sander long ago (Soundararajan, Ravi Kumar, Murugesan, & Chandrashekar, 2016). The rare wood is used externally for the treatment of diabetes, eye and blood diseases, skin diseases, chronic dysentery, headaches and as an aseptic salve, among others. In addition, *P. santalinus* is used to treat leprosy, bone fractures, scorpion stings, swallowing cough and snake bites (Saradamma, Hymavathi, Varadacharyulu, & Damodara, 2016). The heartwood has been highly valued in China and Japan for thousands of years and is used to produce handicrafts, furniture and musical instruments (Navada & Vittal, 2014). In addition to dyeing textiles, medicine and food, the red pigments from the heartwood play an even more important role today as dye sensitizers in solar cells (Krishnaswamy & Sundaresan, 2012).

3.1.3 Known Compounds from Literature

Phytochemical studies of *P. santalinus* show the presence of many different constituents, such as carbohydrates, steroids, anthocyanins, saponins, tannins, triterpenoids, phenolic compounds, glycosides and glycerides (Mohammad, Rajkapoor, & Kavimani, 2015). The heartwood contains the santalins A, B, AC and Y and the santarubins A and B, a series of important insoluble or poorly soluble, strongly coloring pigments, which could be separated to a large extent in the course of this diploma thesis (Arunkumar & Joshi, 2014; Strych & Trauner, 2013; Strych et al., 2015). Table 1 gives an overview of the reported pigments isolated from the heartwood of *P. santalinus.* Further important constituents from the heartwood described in literature are the following: sesquiterpenes (such as pterocarpol, pterocarptriol, isopterocarpolone, pterocarpodiolone, β-eudesmol, cryptomeridiol, canusesnol K and L); flavonoids; isoflavones; isoflavone glycosides; neoflavonoids; benzofurans; auronic glycosides; lignans and stilbene derivatives (Kumar, Ravindranath, & Seshadri, 1974; Li, et al., 2018; Jung, Jeon, Ahn, Kim, & Kim, 2012; Wu, et al., 2011; Kesari, Gupta, & Watal, 2004; Cho, et al., 2001).

Table 1: Reported wood dyes known from literature

Substance class	Substance Name	CAS Registry Number	Structure	MW g/mol
Benzoxanthenon derivates	Santalin A	38185-48-7	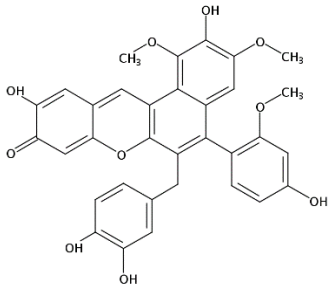	582.55
	Santalin B	51033-46-6	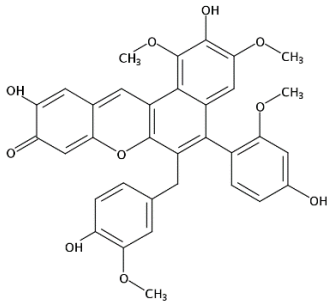	596.58
	Santarubin A	65984-91-0	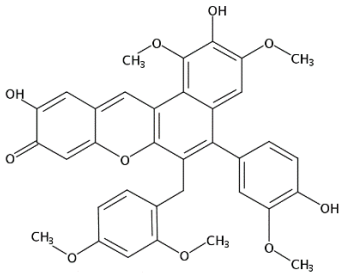	610.61
	Santarubin B	37381-57-0	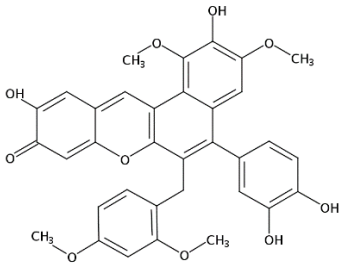	596.58
Isoflavonoid	Santalin AC	167425-76-5	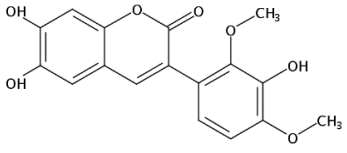	330.29
Oxafenestran	Santalin Y	167425-77-6	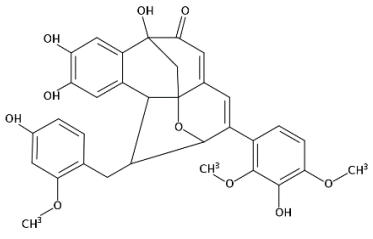	586.59

3.1.4 Reported Bioactivities of Extracts and Pure Compounds from *Pterocarpus santalinus*

3.1.4.1 Radical-scavenging and antioxidant activity

Studies have shown that the methanolic extract prepared from the heartwood of *P. santalinus* has Fe^{3+}-reducing capacity and 2,2-diphenyl-1-picrylhydrazyl (DPPH) radical scavenging activity. Flavonoids and polyphenolic compounds present in the extract are further suggested to be responsible for an observed antioxidant and anti-inflammatory effect (Kumar D. , 2011). It has also been reported that pterostilbene, a structural analog of resveratrol, has antioxidant, anticancer, antidiabetic, and hypolipidemic activities (Remsberg, et al., 2008).

3.1.4.2 Antibacterial activity

The antibacterial activity of the leaf and stem bark extract of *P. santalinus* against Gram-positive bacteria (e.g., *Enterobacter aerogenes*, *Alcaligenes faecalis*, *Escherichia coli*, *Pseudomonas aeruginosa*) was demonstrated, with the extract prepared from the stem bark of Red Sanders showing greater inhibitory activity than the leaf extract (Manjunatha, Antibacterial Activity of Pterocarpus santalinus, 2006). In addition, the leaf extract showed high inhibitory activity against uropathogenic bacteria in contrast to 20 other timber-yielding plants tested, such as e.g., the bark extract of *Pterocarpus marsupium* or the leaf extract of *Eucalyptus citriodora* (Mishra & Padhy, 2013).

3.1.4.3 Anti-inflammatory and cytotoxic effect

Savinin and calocedrin, two lignans isolated from *P. santalinus* heartwood, were shown to significantly inhibit tumor necrosis factor alpha (TNF α) production in lipopolysaccharide stimulated RAW264.7 cells (Cho, et al., 2001). It was also found that the methanolic extract showed significant cytotoxic activity and induction of apoptosis on HeLa cells, a human cervical adenocarcinoma cell line (Kwon, et al., 2006). The phenanthrendione pterolinus K and the chalcone pterolinus L, both isolated from the heartwood of *P. santalinus*, showed anti-inflammatory activity and cytotoxicity against human cancer cell lines (HepG2, Hep3B, A549) (Wu, et al., 2011). The benzofurans Pterolinus A-E and the neoflavonoids Pterolinus F-J exhibit potent anti-inflammatory activity, whereas melanoxoin, also a benzofuran compound isolated from the heartwood extract additionally exhibits cytotoxicity against Ca9-22 cancer cells with an IC_{50} value of 0.5 µg/mL (Wu, et al., 2011).

3.1.4.4 Antidiabetic & Hypolipidemic Activity

Phytochemical studies have shown that the substances sitosterol, lupeol, and (-)-epi-catechin contained in the bark of *P. santalinus* show hypoglycemic and antihyperglycemic activity (Kameswara Rao, Giri, Kesavulu, & Apparao, 2001). Studies in streptozoticin-induced diabetic rats demonstrated that (i) consituents from the ethanolic extract of *P. santalinus* have antihyperglycemic and antihyperlipidemic effects by improving insulin secretion and altering carbohydrate and lipid metabolism (Kondeti, et al., 2010), and (ii) the combination of an aqueous extract with vitamin E significantly reduces blood glucose levels ($p < 0.001$), improves glucose tolerance ($p < 0.001$) and significantly reduces serum lipids and body weight ($p < 0.001$) compared to non-treated diabetic rats (Halim & Misra, 2011).

3.1.4.5 Other pharmacological uses

P. santalinus additionally shows hepatoprotective, gastroprotective, and wound-healing properties, which have been demonstrated in different studies each on Wistar albino rats:

1. Both, the ethanolic and aqueous stem bark extract of *P. santalinus* provides significant protection against CCl_4-induced hepatocellular injuries (Manjunatha, 2006)
2. An ethanolic heartwood extract (150 mg/kg body weight/day) was found to be gastroprotective against ibuprofen-induced ulcers by leading to a significant reduction in gastric lesions, an increase in antioxidant enzyme activities, and a decrease in membrane-bound ATPase activities (Narayan, Devi, Srinivasan, & Shyamala Devi, 2005)
3. A salve prepared from the powder wood of *P. santalinus* allows acute wounds to heal significantly faster compared to the untreated control (Biswas, Maity, & Mukhherjee, 2004).

3.2 Phenotypic Screening of Selected Samples Affecting the Health Span of *Caenorhabditis elegans*

3.2.1 Aging and Aging-Related Diseases

Aging is a complex, multifactorial process of molecular and cellular deterioration that affects tissue and organ function over time, leaving the organism vulnerable to disease and death (Carmona & Michan, 2016). By 2050, the proportion of people aged 60 or older is expected to be higher than the proportion of teenagers and young adults combined for the first time in human history. The main reasons are improved nutrition, living conditions, sanitation, and health care in modern days. Concurrently, aging is considered to be the biggest risk factor for most common chronic human diseases, such as cardiovascular disease, cancer, dementia, diabetes, osteoarthritis or osteoporosis. Therefore, strategies and new therapeutic pathways that target the conserved molecular and cellular mechanisms of aging, as opposed to treating each individual age-associated disease, could slow the process of aging and have a tremendous effect on global health (Zhang, et al., 2020).

3.2.1 *Caenorhabditis elegans* as a model Organism for Aging Research

Caenorhabditis elegans (*C. elegans*) is a free-living nematode and has been one of the most important animal models for aging research for decades. Compared to other animal models, *C. elegans* has many advantages, such as a small body size, a short lifespan and reproductive cycle, and a fully sequenced genome with more than 65% of the genes associated with human diseases (Shen, Yue, & Park, 2018). Most genes and interventions that modulate aging, such as the insulin/insulin-like growth factor-1 signaling pathway, mitochondrial signaling, and caloric restriction, were first identified in this organism. It is known that genes regulating the aging process in *C. elegans* are evolutionarily conserved and their deregulation is implicated in the development of age-associated diseases. Therefore, it is likely that interventions leading to lifespan extension in *C. elegans* will provide targets for lifespan extension strategies in humans (Torgovnick, Schiavi, Maglioni, & Ventura, 2013). Previously, a miniaturized, medium throughput platform was established at the Division of Pharmacognosy with a main focus on natural products, such as extracts, fractions and isolated compounds (Zwirchmayr, et al., 2020) and was accordingly used for wild type as well as genetically modified *C. elegans* strains.

3.2.1.1 The Role of Oxidative Stress in Aging

Oxidative stress is assumed to be an important mechanism limiting longevity in general but also limiting the health longevity in particular. Several age-related pathologies, such as cardiovascular and neurodegenerative diseases, cancer and diabetes have been related to oxidative stress. All aerobic organisms, from unicellular organisms to humans, are always exposed to oxidants and electrophiles. On the one hand, through endogenous oxidants generated by enzymatic processes, for example in the electron transport system in mitochondria, and on the other hand, through exogenous pollutants, such as radiation exposure, high-fat diet, cigarette smoke and alcohol consumption. To avoid the harmful effects of these oxidative agents (which occurs at higher levels), the organism has evolved an antioxidant system to maintain redox homeostasis. Oxidative stress occurs when the oxidant/antioxidant balance is disturbed and shifted toward the oxidants, resulting in disruption of redox signaling and molecular damage. With age, the organism becomes more vulnerable to oxidants and other toxins, and at the same time antioxidant defense decreases, leading to oxidative damage to proteins, nucleic acids and lipids in aging cells (Vatner, et al., 2020; Zhang, Davies, & Forman, 2015).

3.2.1.2 The Role of the mammalian Transcription Factor FOXO3 in Aging

The insulin/IGF-1 signaling (IIS) pathway is an evolutionarily conserved signaling pathway that regulates aging across various species, from the invertebrate *C. elegans* to mammals. FOXO proteins, as part of the Forkhead family (Forkhead box O), are the major transcriptional effectors of IIS and influence aging and age-related diseases. Mammals have four FOXO genes that are involved in a variety of important cellular processes, including stress resistance, metabolism, cell cycle arrest, and apoptosis (Martins, Lithgow, & Link, 2016). Different studies suggest that genetic variants in FOXO3 transcription factor contribute to achieving old age, but future studies are needed to demonstrate the role of FOXO3 in healthy aging (Torgovnick, Schiavi, Maglioni, & Ventura, 2013).

3.2.1.2.1 The Ortholog *daf-16* in *Caenorhabditis elegans*

In *C. elegans*, the IIS pathway comprises an insulin-like receptor (*daf-2*) that switches *daf-16* downstream, the ortholog of the mammalian transcription factor FOXO (Back, Braeckman, & Matthijssens, 2012). It has been found that a mutation in the *daf-2* gene causes *daf-16* specific longevity genes to be activated, thereby doubling the lifespan of *C. elegans* (Martins, Lithgow, & Link, 2016). On the other hand, mutations in *daf-16* may cause suppression of the longevity effects of *daf-2* mutants (Torgovnick, Schiavi, Maglioni, & Ventura, 2013).

3.2.1.3 The Role of the mammalian Transcription Factor NF-E2-related Factor 2 (Nrf2)

The mammalian nuclear factor erythroid 2-related factor 2 (more commonly known as Nrf2) is by far the best studied transcription factor of the Nrf family, responsible for the expression of hundreds of antioxidant and detoxifying enzymes including the proteasome. The Nrf2 signaling system is among the most important cellular defenses against oxidative stress and toxins; therefore, disruption of Nrf2 signaling results in increased vulnerability to oxidative stress and other toxins (Zhang, Davies, & Forman, 2015).

3.2.1.3.1 The Ortholog *skn-1* in *Caenorhabditis elegans*

In *C. elegans*, the Nrf proteins are represented by their ortholog *skn-1*. *Skn-1* plays a central role in many regulatory pathways that extend lifespan. It is known that *skn-1* promotes longevity in wild type animals and that loss-of-function *skn-1* mutants have a shortened lifespan. In addition, constitutive expression of many *skn-1*-regulated genes declines with age, resulting in loss of defense against oxidative stress (Blackwell, Steinbaugh, Hourihan, Ewald, & Isik, 2015).

4 RESULTS AND DISCUSSION

4.1 Isolation and Characterization of Bioactive Constituents from *Pterocarpus santalinus* affecting the Health Span of *Caenorhabditis elegans*

4.1.1 Phytochemical Workflow of the Large-Scale Extract PtesanXDM_LS

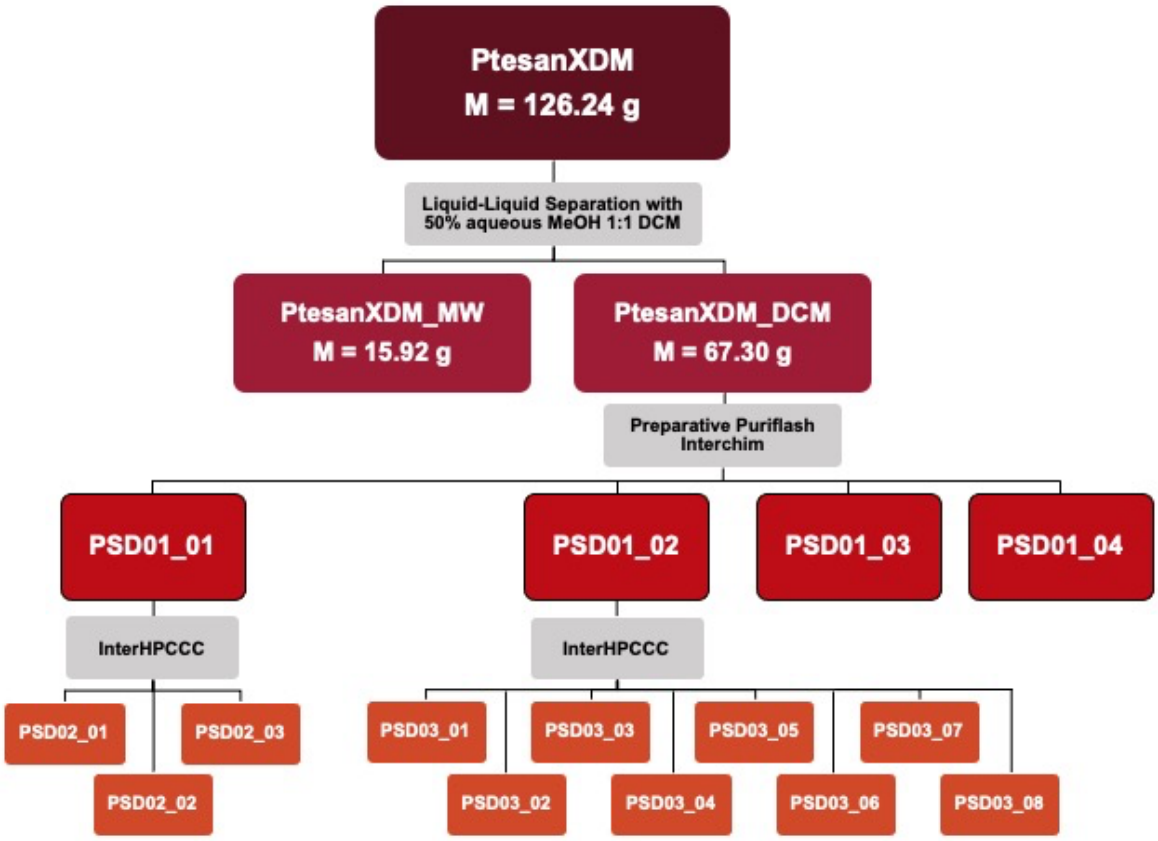

Figure 3: Fractionation tree of PtesanXDM_LS

4.1.2 Liquid-Liquid Separation of PtesanXDM_LS

All preliminary experiments as well as the subsequent large-scale liquid-liquid separation were performed using the large-scale lead-like enhanced extract prepared from the heartwood of *P. santalinus* (i.e. PtesanXDM_LS, i.e. PresanXDM in Figure 3), since an extensive amount of this extract was available. Before a further separation of the extract was carried out using PuriFlash Interchim, a liquid-liquid separation was executed to deplete the highly staining pigments contained in the extract. Therefore, the extract was separated between two immiscible solvent phases of different density in a separating funnel. The substances in the extract distribute into the solvent in which they dissolve better. In order to find a suitable biphasic solvent system for the depletion of pigments contained in PtesanXDM_LS, the following solvent systems were tested:

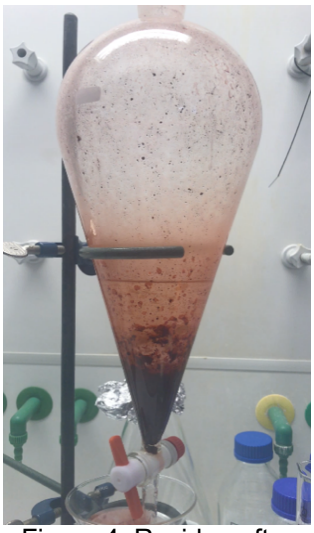

Figure 4: Residue after separation with PE and H_2O

For the first liquid-liquid separation, petroleum ether (PE) was used as the non-polar organic solvent and water as the polar aqueous solvent. About 8 g of PtesanXDM_LS were suspended in 10 ml of water in an ultrasonic bath and then transferred to a 2 liter separating funnel. Undissolved “chunks” of the extract were loosened with a spatula, then suspended with 10 ml of PE and also transferred to the separating funnel. After shaking out with a total of 500 ml of water (H_2O) and 500 ml of PE, the two phases were collected in separate round bottom flasks and evaporated on the rotary evaporator under reduced pressure. This process was repeated in total four times. Unfortunately, most of the crude extract did not dissolve in either PE or H_2O but remained undissolved in the separating funnel (Figure 4). Therefore, the separation with PE and H_2O was not feasible. The undissolved extract was then dissolved with methanol (MeOH) and transferred back to the crude extract PtesanXDM_LS.

To obtain a sufficient depletion of the pigments, a second liquid-liquid separation was performed with another biphasic solvent system. For this procedure, a MeOH-H_2O mixture was used as polar aqueous solvent and dichloromethane (DCM) as nonpolar organic solvent. Small-scale experiments were performed in a 25 ml separatory funnel. MeOH and H_2O were mixed in ratios of 30:70, 50:50, and 70:30, respectively. The ratio of polar solvent to nonpolar solvent on the other hand varied from 1:1 and 2:1. The best result was obtained with the 50% aqueous MeOH as the aqueous solvent and DCM as the organic solvent in the ratio 1:1, since:

1. no residue of the extract remained in the separating funnel
2. the phase separation was still clearly visible after shaking out and
3. according to the thin layer chromatogram (TLC), a large part of the pigments could be separated into the MeOH-H_2O phase.

Thereafter, a large scale separation as described above was performed using the DCM-50% aqueous MeOH (MW) solvent system in a 2 liter separatory funnel (Figure 5). A total of ~ 85 g PtesanXDM were separated in 16 cycles. For each cycle, 500 ml of polar and 500 ml of nonpolar solvent were used. To keep solvent consumption as low as possible, solvents were recycled by evaporating the fractions on the rotary evaporator and re-used for the next liquid-liquid separation. With this large scale separation, 67.3 g of PtesanXDM_DCM and 15.9 g of PtesanXDM_MW were obtained. An overview of the detailed liquid-liquid separation process is shown in Figure 27 in Chapter 6.1.2.

Figure 5: Liquid-Liquid separation with MW:DCM

4.1.2.1 UPLC of Liquid-Liquid Separation Fractions PtesanXDM_LS, PtesanXDM_DCM and PtesanXDM_MW

The used method for the separation is shown in Table 21 in Chapter 6.1.4.5. The corresponding UHPLC chromatogram is given in Figure 6. In the upper panel the chromatogram of PtesanXDM_LS prior to any liquid-liquid separation is shown. The second panel shows the pigment-depleted fraction (i.e. PtesanXDM_DCM) whereas the third panel shows the pigment-enriched fraction (i.e. PtesanXDM_MW). A TLC of PtesanXDM_LS, PtesanXDM_DCM and PtesanXDM_MW was performed and confirmed the successful depletion of the persistend pigments (chromatogram not shown).

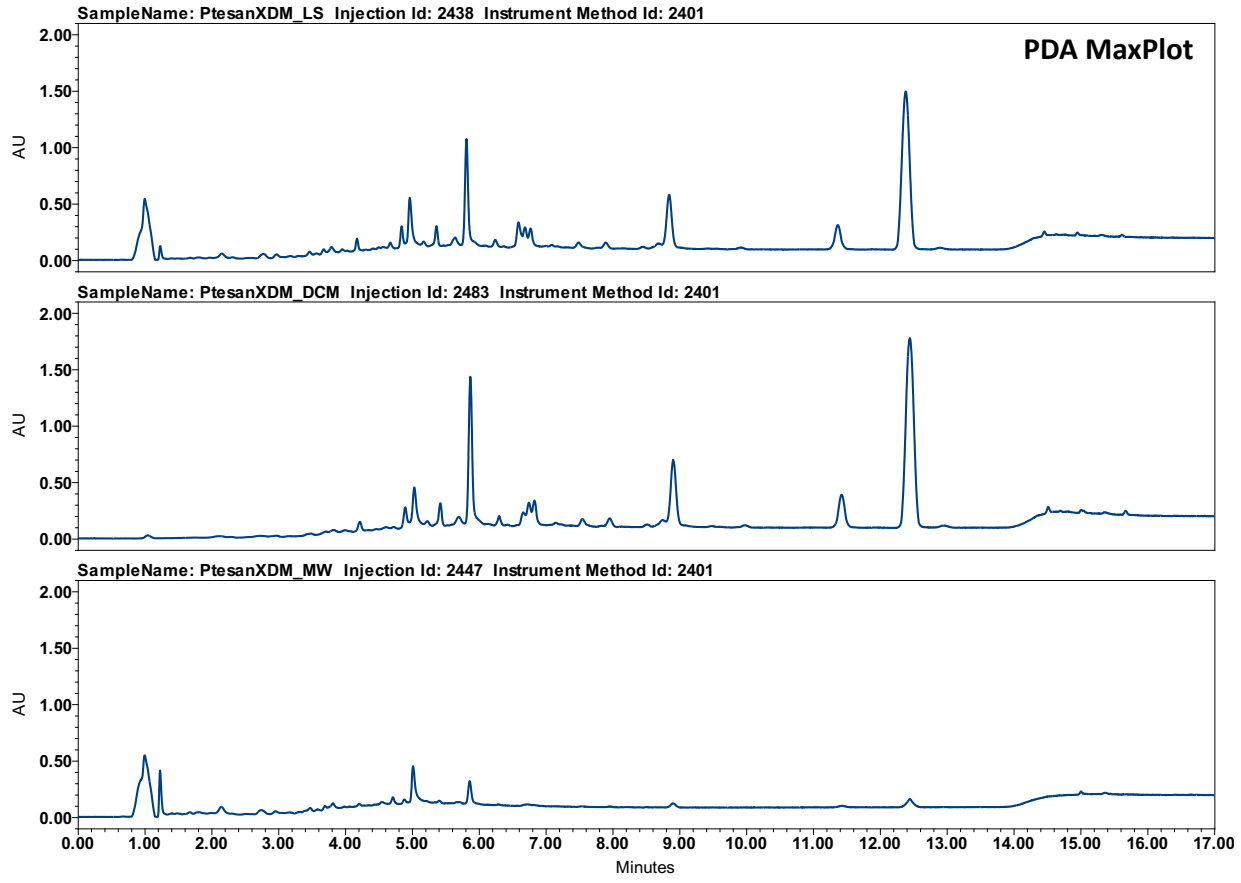

Figure 6: UHPLC chromatogram of fractions PtesanXDM_LS, PtesanXDM_DCM and PtesanXDM_MW; Channel: PDA 210 nm

4.1.2.2 *C. elegans* Lifespan Assay of PtesanXDM_LS, PtesanXDM_DCM and PtesanXDM_MW

In order to keep track of the lifespan prolonging activity of PtesanXDM_LS, a bioactivity guided fractionation procedure was performed. Hence, each fraction obtained during the phytochemical work-up of PtesanXDM_LS was monitored and evaluated in the *C. elegans* lifespan assay. Figure 7 and Table 2 shows the results of the *C. elegans* lifespan assay with wilde-type worms (N2). PtesanXDM (=PtesanXDM_LS), the pigment-depleted DCM-fraction (PtesanXDM_DCM) and the pigment-enrichted MW fraction (PtesanXDM_MW) were tested at 25 and 10 µg/mL using the anti-hypertensive drug reserpine at 30 µM as positive control. As it can be seen, reserpine significantly delays the time-point when 50% of the nematodes were dead (= death-time 50%; DT_{50}) by 45.6% ($p < 0.01$). The lead-like enhanced large-scale extract PtesanXDM_LS as well as the DCM-fraction PtesanXDM_DCM show significant lifespan prolonging effects at 10 µg/mL with a DT_{50} extension of 32.9% and 52.3%, respectively. The higher concentration of both samples as well as the pigment-depleted fraction PtesanXDM_MW (both concentrations) showed no activity ($p > 0.05$). Unsurprisingly the secondary metabolites with a lifespan prolonging activity are enriched in PtesanXDM_DCM. Hence, this sample was further phytochemically investigated.

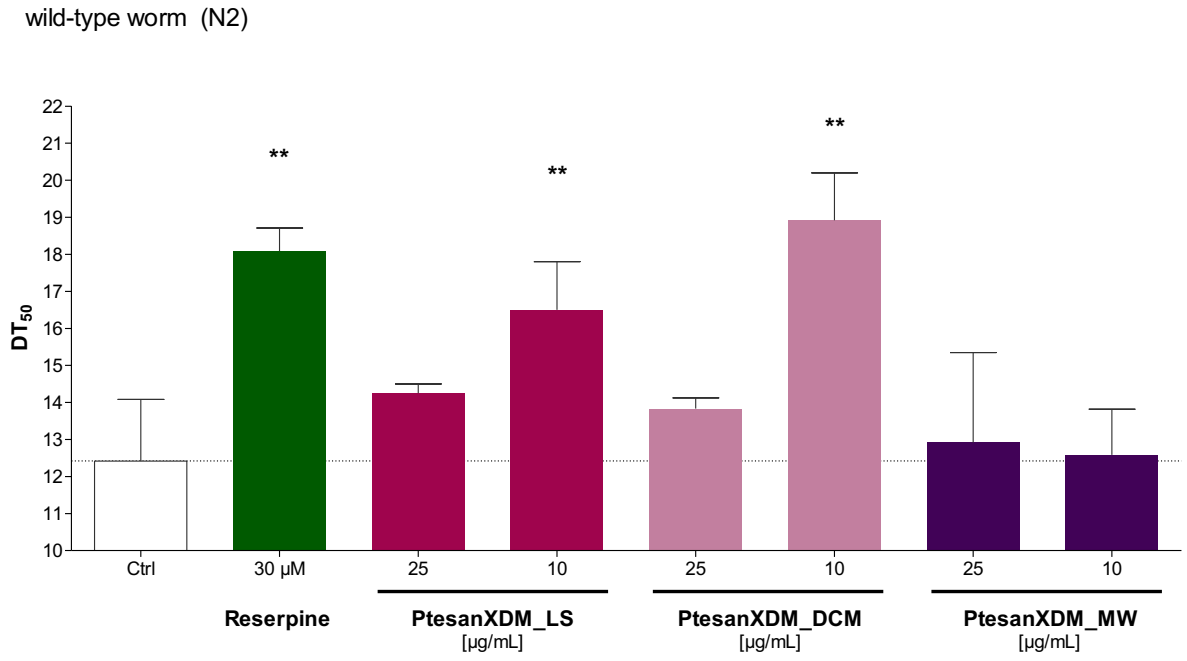

Figure 7: Results of a *C. elegans* Lifespan Assay with N2 wild-type worms; The crude extract PtesanXDM, the pigment-depleted fraction PtesanXDM_DCM, the pigment-rich fraction PtesanXDM_MW (all at 25 and 10 µg/mL), the vehicle control (DMSO 1%) and the positive control reserpine 30 µM were assayed for lifespan prolonging effects. Bars represent the mean DT_{50} ± SD of three parallel experiments. Significance was assessed by One-Way ANOVA with Dunnett's post-test (*p < 0.05; **p < 0.01).

Table 2: Survival analysis upon treatment with PtesanXDM_LS, PtesanXDM_DCM and PtesanXDM_MW. One way ANOVA with Dunnett's post-test was used for statistical evaluation. P-value < 0.05 was considered as statistically significant.

Sample	*c*	Mean DT_{50} ± SD	DT_{50} extension (%)	*p*-value
Control	-	12.42 ± 1.67	-	-
Reserpine	30 µM	18.08 ± 0.63	45.57	***p* < 0.01**
PtesanXDM_LS	25 µg/mL	14.25 ± 0.25	14.73	*p* > 0.05
	10 µg/mL	16.50 ± 1.30	32.85	***p* < 0.01**
PtesanXDM_DCM	25 µg/mL	13.83 ± 0.29	11.35	*p* > 0.05
	10 µg/mL	18.92 ± 1.28	52.33	***p* < 0.01**
PtesanXDM_MW	25 µg/mL	12.92 ± 2.43	4.03	*p* > 0.05
	10 µg/mL	12.58 ± 1.23	1.29	*p* > 0.05

4.1.3 Preparative Fractionation of PtesanXDM_DCM with Puriflash Interchim

PtesanXDM_DCM extract obtained by liquid-liquid separation was further fractionated using PuriFlash Interchim. Stationary phase silica columns and reversed phase columns were tested with different solvent systems and solvent gradients in preliminary experiments (Table 12 in Chapter 6.1.4.1). PuriFlash Interchim was the method of choice since a large sample volume, 10.206 g to be exact, could be separated by a huge stationary column within one preparative run. Sample delivery was performed by dry load application (Figure 8). Normal phase chromatography was chosen for the preparative fractionation of PtesanXDM_DCM as the TLC of the analytical methods showed a better separation in the normal phase mode. In addition, the extracts obtained were easier to process due to the volatile mobile phase. The method used for preparative fractionation is shown in Table 13 in Chapter 6.1.4.1. The resulting 442 fractions were analyzed by TLC and similar fractions were combined, finally obtaining 4 fractions, namely PSD01_01 – PSD01_04. Further, these fractions were analyzed by UPLC. Which fractions were combined and the yields of the combined fractions PSD01_01 – PSD01_04 are shown in Table 14 in chapter 6.1.4.1.

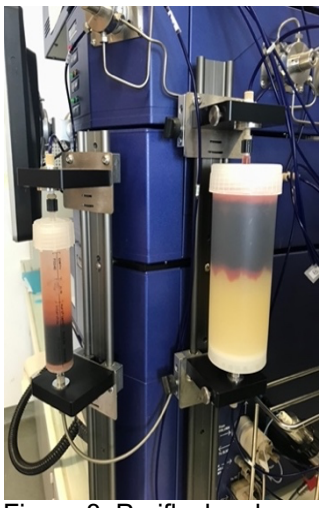

Figure 8: Puriflash column 25 Silica HC 200 G

4.1.3.1 TLC of Interchim Fractions PSD01_01 to PSD01_04

The resulting PuriFlash Interchim fractionations PSD01_01 – PSD01_04 and the large-scale extract PtesanXDM_DCM were analyzed by collective-TLC (Figure 9). TLC parameters are described in Chapter 6.1.4.4. As it can be seen, all of the polar pigments are distributed between the fractions PSD01_03 and PSD01_04, whereas PSD01_04 contains the vast majority.

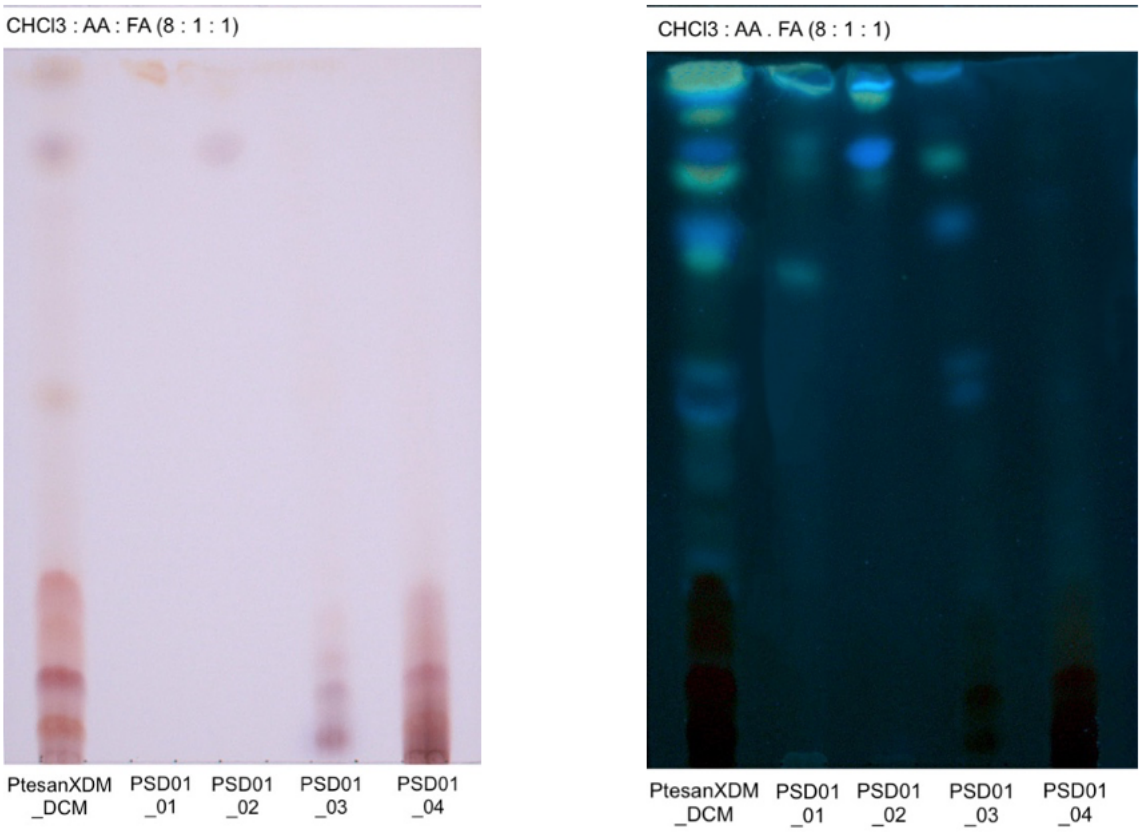

Figure 9: Collective-TLC analysis of fractions PtesanXDM_DCM, PSD01_01 - PSD01_04; left: Detection in VIS after using spraying reagent vanillin/sulphuric acid, right: Detection at UV366 nm

4.1.3.2 UPLC of Interchim Fractions PSD01_01 to PSD01_04

Further, the resulting PuriFlash Interchim fractions PSD01_01 – PSD01_04 were analyzed by UHPLC (Figure 10). The first panel shows the pigment-depleted fraction PtesanXDM_DCM, in panel two – five the Interchim fractions PSD01_01 – PSD01_04 are shown. UHPLC parameters are described in Table 21 in Chapter 6.1.4.5.

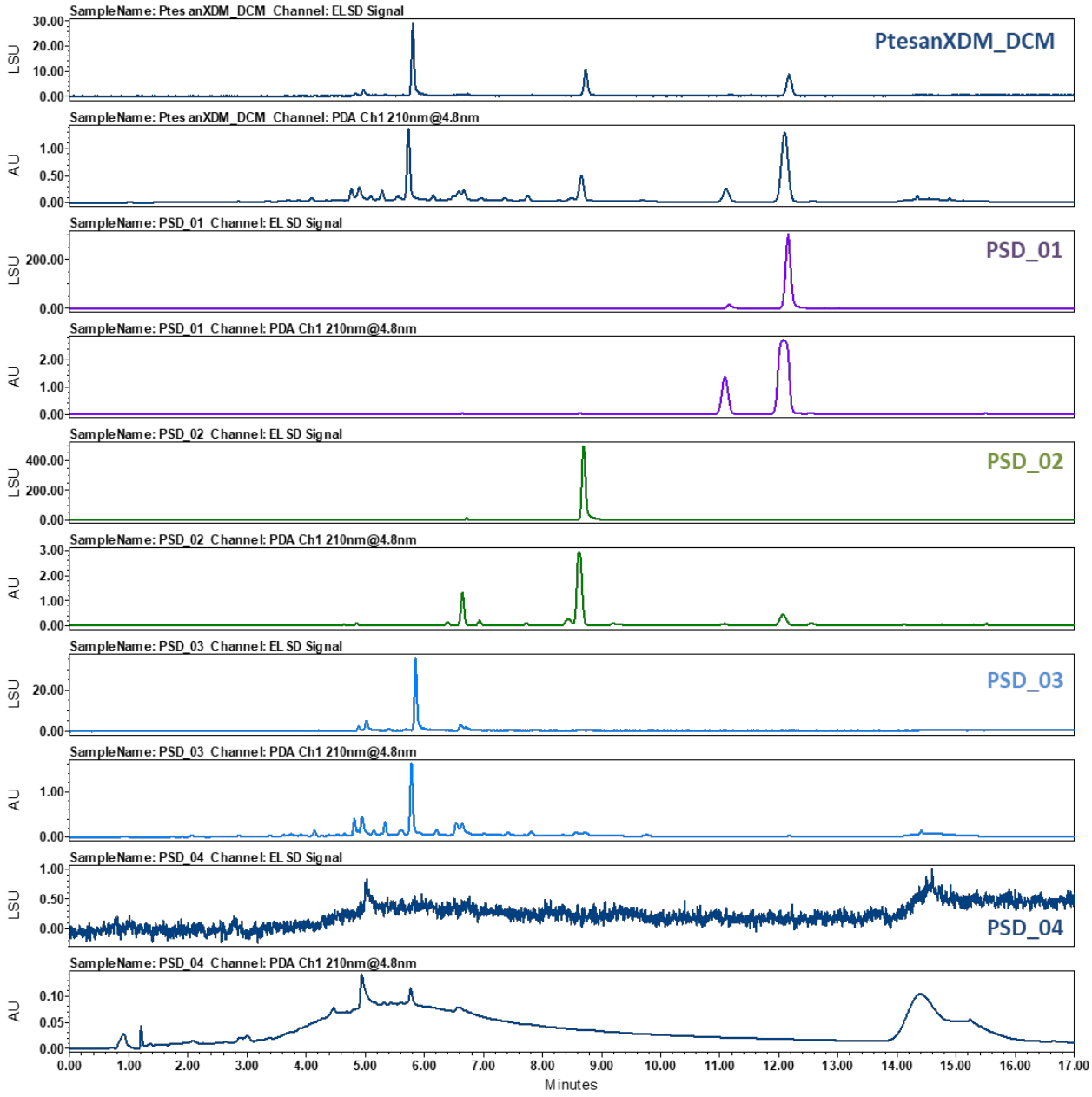

Figure 10: UHPLC chromatogram of Interchim fractions PtesanXDM_DCM and PSD01_01 – PSD01_04; Channel: ELSD (upper) and PDA 210 nm (lower panel)

4.1.3.3 *C. elegans* Lifespan Assay of the Interchim Fractions PSD01_01 – PSD01_04

Again, all fractions generated with the Puriflash Interchim were assayed in the *C. elegans* lifespan assay at 25 and 10 µg/mL. The results of the screening are shown in Figure 11 and Table 3. Apart from the positive control reserpine, PSD01_03 extended the mean survival rate of the nematodes by 36.9% and 36.2% (at 25 and 10 µg/mL; both $p < 0.05$) when compared to the untreated control. Interestingly, PSD01_02 at 25 µg/mL significantly decreased the DT_{50} value by 31.6%. This detrimental effect on the nematodes survival completely vanished at the lower concentration of 10 µg/mL resulting in hardly any effects on the worm's survival (DT_{50} extension ~ 4%). Likewise, the pigment-enriched fraction PSD01_04 showed slightly – hardly any effects on the lifespan of *C. elegans* with a DT_{50} reduction of 21.5% and 7.4% at 25 µg/mL and 10 µg/mL, respectively. At 10 µg/mL PSD01_01 resulted in a DT_{50} extension of 19.4% (however, not significantly). Altogether, this screening showed interesting results regarding bioactivity gathering in the respective fractions, not only in terms of lifespan extension but also lifespan shortening (e.g. anti-helminthic properties). For reasons of time, the most active fraction PSD01_03, which incidentally is also the most complex fraction, was not further investigated within the scope of this thesis. Instead, PSD01_01 and PSD01_02 were further investigated with a newly developed technique combining the Puriflash Interchim with the High-Performance Counter-Current Chromatography (HPCCC) device.

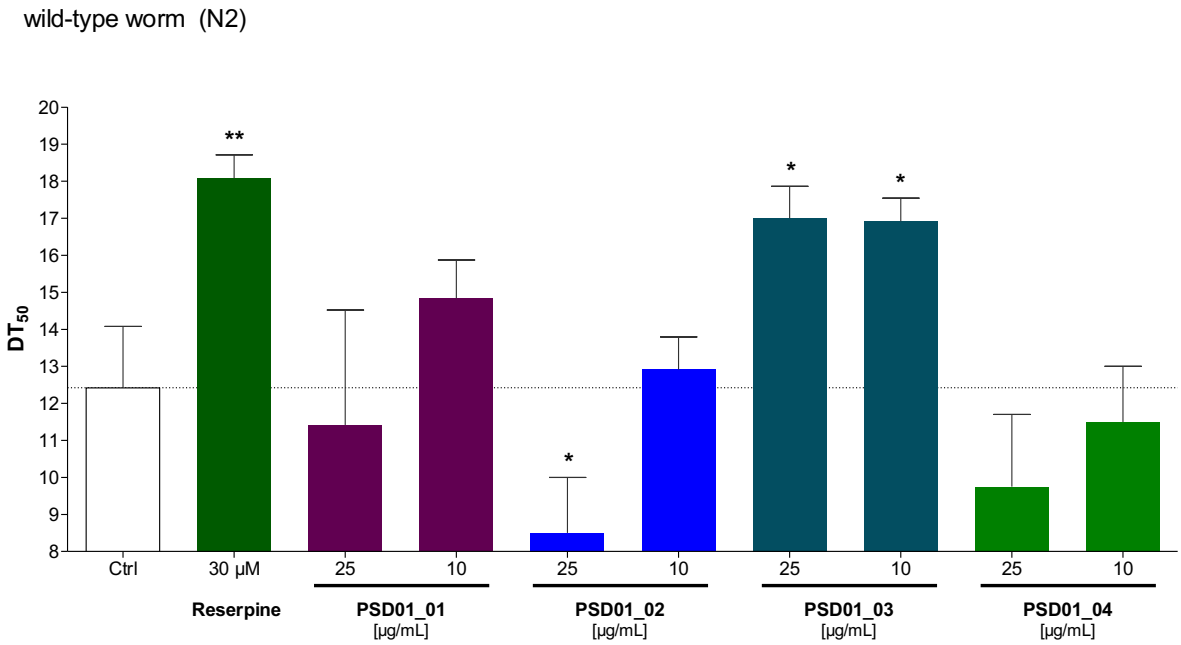

Figure 11: Results of a *C. elegans* Lifespan Assay with N2 wild-type worms; The puriFlash Interchim fractions PSD01_01 – PSD01_04 (all at 25 and 10 µg/mL), the vehicle control (DMSO 1%) and the positive control reserpine 30 µM were assayed for lifespan prolonging effects. Bars represent the mean DT_{50} ± SD of three parallel experiments. Significance was assessed by One-Way ANOVA with Dunnett's post-test (*p < 0.05; **p < 0.01).

Table 3: Survival analysis upon treatment with the Puriflash Interchim fractions PSD01_01 – PSD01_04. One way ANOVA with Dunnett's post-test was used for statistical evaluation. P-value < 0.05 was considered as statistically significant.

Sample	*c*	Mean DT_{50} ± SD	DT_{50} extension (%)	*p*-value
Control	-	12.42 ± 1.67	-	-
Reserpine	30 µM	18.08 ± 0.63	45.57	***p* < 0.01**
PSD01_01	25 µg/mL	11.42 ± 3.10	-8.05	*p* > 0.05
	10 µg/mL	14.83 ± 1.04	19.40	*p* > 0.05
PSD01_02	25 µg/mL	8.50 ± 1.50	-31.56	***p* < 0.05**
	10 µg/mL	12.92 ± 0.88	4.03	*p* > 0.05
PSD01_03	25 µg/mL	17.00 ± 0.87	36.88	***p* < 0.05**
	10 µg/mL	16.92 ± 0.63	36.23	***p* < 0.05**
PSD01_04	25 µg/mL	9.75 ± 1.95	-21.50	*p* > 0.05
	10 µg/mL	11.50 ± 1.50	-7.41	*p* > 0.05

4.1.4 Semi-Preparative Fractionation of PSD01_01 with Interchim-High-Performance Counter-Current Chromatography

After preparative separation of PtesanXDM_DCM using puriFlash Interchim, the resulting fraction PSD01_01 was further fractionated using HPCCC. HPCCC was the method of choice as it offers many advantages, in particular the possibility of (i) up-scaling the process from an analytical do semi-preparative performance, hence applying large sample volumes (up to 450 mg), (ii) adjusting the solvents for the fractionation to the given polarity of each sample by using different solvent rations of *n*-hexane (*n*-hex), ethyl acetate (EtOAc), MeOH and H_2O (HEMWat) and (iii) avoiding loss of substance by adsorption to any stationary solid column.

Initially, a suitable solvent system for HPCCC fractionation was sought for PSD01_01. Solvent system screening was performed as follows: ~ 2 mg of PSD01_01 were dissolved in 2.0 ml EtOAc (stock solution, SSo). Since the fraction PSD01_01 contains rather non-polar constituents, mixtures of the also non-polar HEMWat-systems 17, 19, 21, 23 and 25 were prepared (Table 15 in Chapter 6.1.4.2). Depending on the HEMWat system, different proportions of *n*-hex, EtOAc, MeOH and H_2O were mixed in a test tube, with one part EtOAc being replaced by one part of the SSo. Shaking the test tube distributed the sample into the resulting two phases. The upper and lower phases of each system were then analyzed by TLC. Separation via HPCCC is best when the constituents have similar affinity for both, the lower and upper phase. To increase the time effectiveness of the HPCCC separation, the HPCCC was coupled with the Interchim PuriFlash. The Interchim device serves as a pump and the HPCCC device serves as a column. For the semi-preparative fractionation of extract PSD01_01, an isocratic normal phase mode using HEMWat solvent system 23 was selected, since the constituents were well distributed between the lower and upper phase. About 1000 ml lower phase and 1000 ml upper phase of HEMWat solvent system 23 were prepared. First, the HPCCC coil was filled with the lower phase of HEMWat system 23 at a flow rate of 10 ml/min and a column rotation of 200 rpm. Once completely filled, the upper phase was pumped into the system at a speed of 1.600 rpm and a flow rate of 6 ml/min. After equilibrium was reached, approximately 70 mg of the fraction, dissolved in 10 ml of the upper phase, was injected. In total, five injections were made in one run, since it was known from the chromatogram of the PDA and ELSD detectors when the compounds were completely separated and eluted from the device(s). Table 16 in Chapter 6.1.4.2 shows the HPCCC method with isocratic elution for the semi-preparative fractionation. A total of 375.2 mg of PSD01_01

extract could be separated. 232 fractions were analyzed by TLC and combined to three final fractions, namely PSD02_01 - PSD02_03 (Figure 12). The yields are shown in Table 17 in Chapter 6.1.4.2.

4.1.4.1 TLC of PSD02_01 to PSD02_03

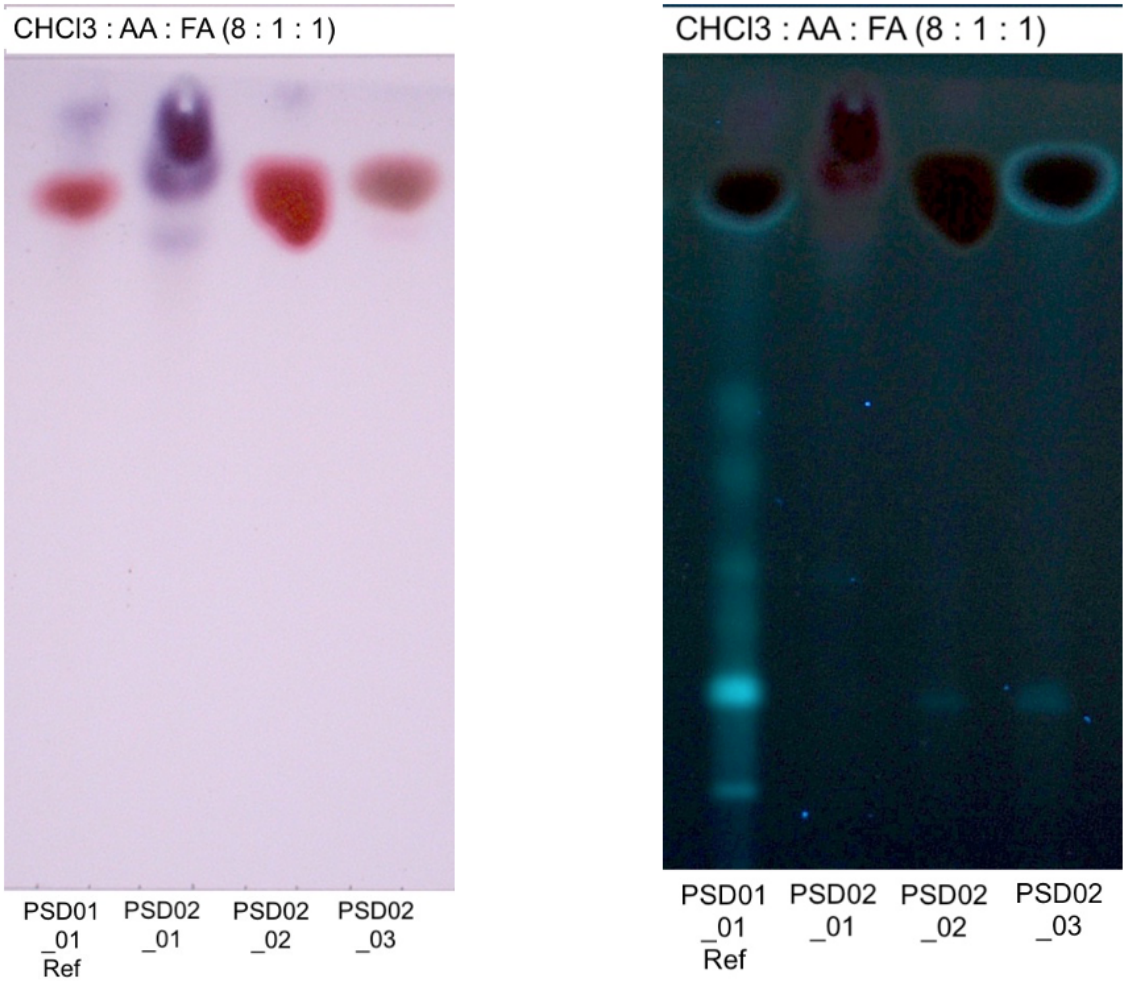

Figure 12: Collective-TLC analysis of HPCCC fractions PSD02_01 - PSD02_03; left: Detection in VIS after using spraying reagent vanillin/sulphuric acid, right: Detection at UV366 nm

4.1.4.2 UPLC of PSD02_01 to PSD02_03

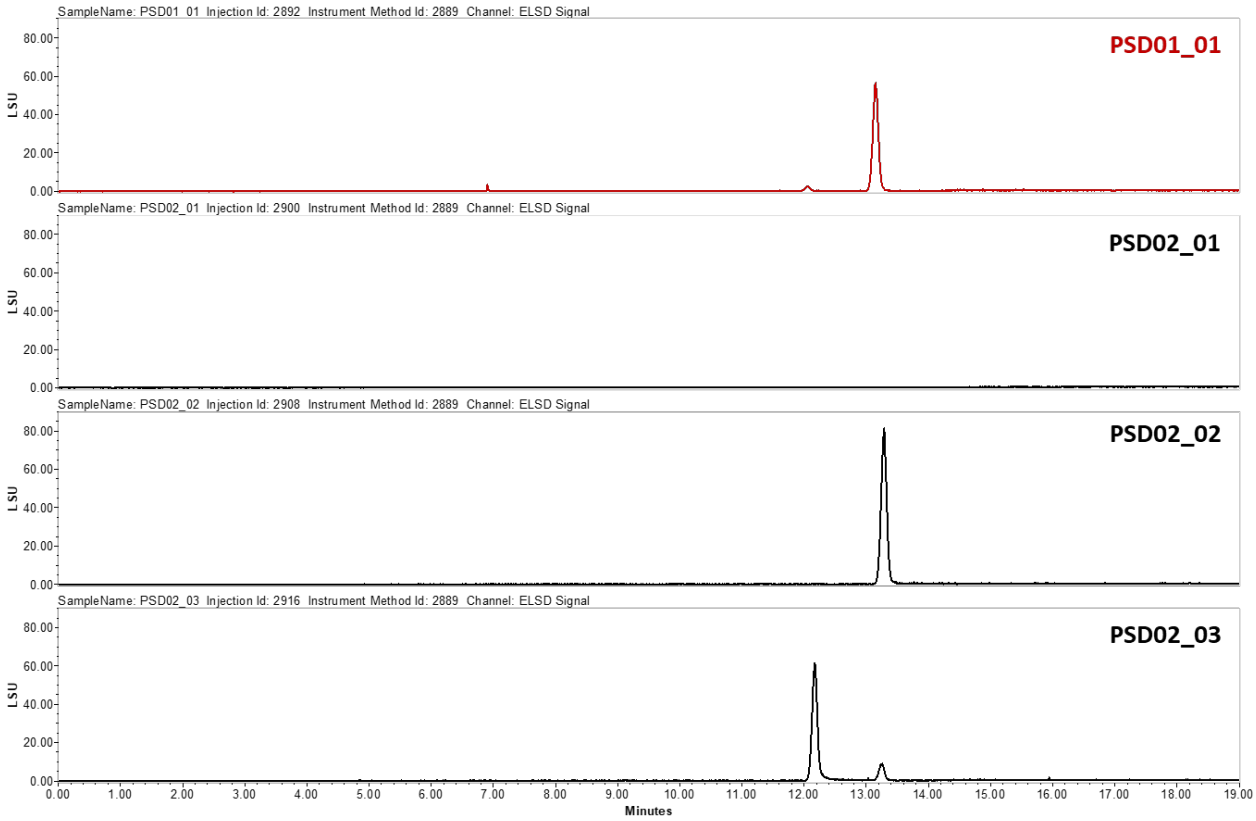

Figure 13: UPLC chromatogram of PSD01_01 and the deriving Interchim-HPCCC fractions PSD02_01 - PSD02_03. *(*ELSD*)*

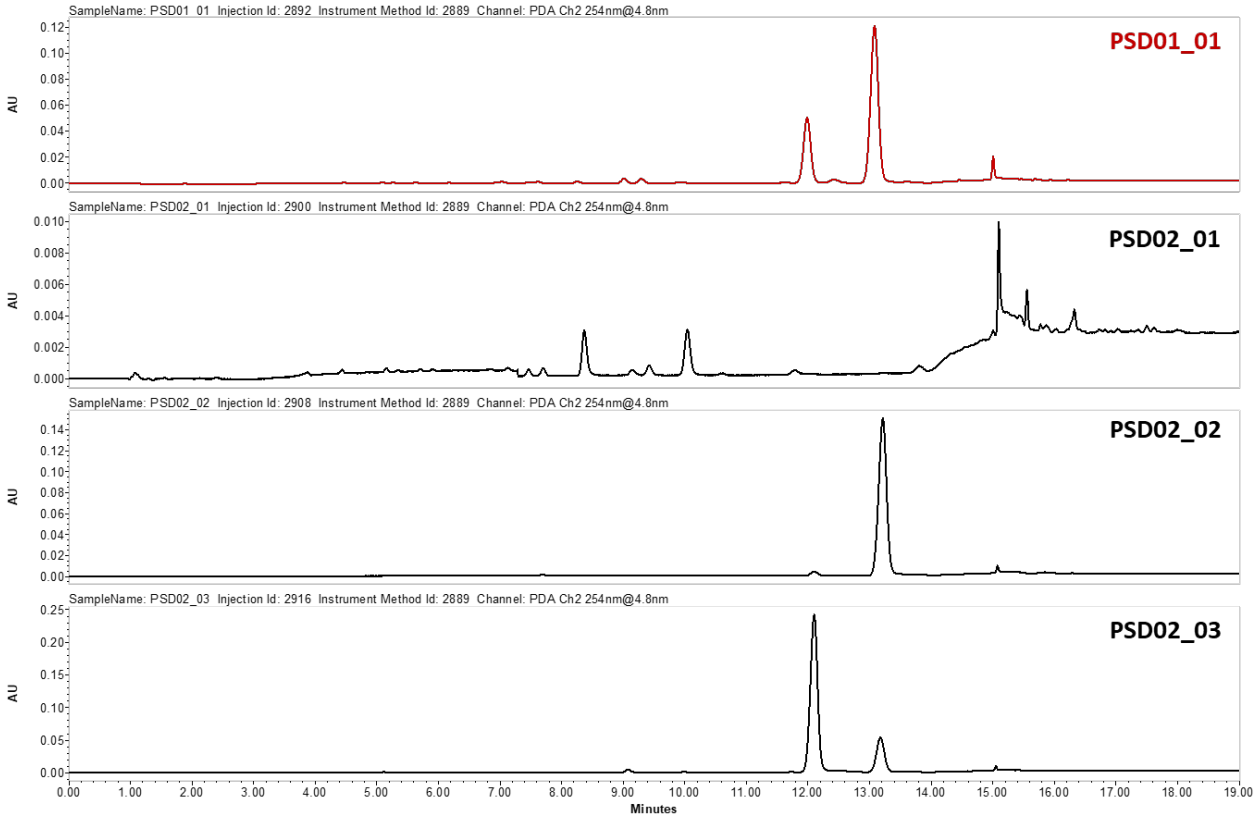

Figure 14: UPLC chromatogram of PSD01_01 and the deriving Interchim-HPCCC fractions PSD02_01 - PSD02_03. (PDA 254 nm)

4.1.5 Semi-Preparative Fractionation of PSD01_02 with Interchim-High-Performance Counter-Current Chromatography

A solvent system-screening was performed according to the same principle as described in the previous chapter. Mixtures of HEMWat systems 15, 17, 18, 19, 20, 21 and 23 were prepared and analyzed by TLC, with the difference that MeOH was used instead of EtOAc to prepare the SSo (Table 18 in Chapter 6.1.4.3). TLC monitoring of the sample's distribution between upper and lower phases of all HEMWat systems showed the best results for the HEMWat systems 23 and 19. Hence, system 23 and 19 were used for the fractionation of PSD01_02. Here, a gradient elution instead of an isocratic elution was used to improve separation efficiency. The HPCCC device was also coupled to the Interchim PuriFlash system. Experiments were initially performed at the analytical scale (flow rate 2 ml/min) and later scaled up using the semi-preparative column (flow rate 6 ml/min). In the semi-preparative run, 269.0 mg of sample could be separated. For the gradient elution the HPCCC coil was first filled with the lower stationary phase of the HEMWat system 23. After setting up the fractionation at 1600 rpm and reaching equilibrium with the upper mobile phase of the HEMWat system 23, PSD01_02 dissolved in 5 mL of mobile and 5 mL of stationary phase was injected. Successively, the upper phase of HEMWat system 19 was pumped through the system with an increasing gradient. Table 19 in Chapter 6.1.4.3 shows the HPCCC method for the semi-preparative fractionation. 193 fractions were analyzed by TLC and combined to eight final fractions, namely PSD3_01 to PSD03_8 (Figure 15 and Figure 16). The yields are shown in Table 20 in Chapter 6.1.4.3.

4.1.5.1 TLC of PSD03_01 to PSD03_08

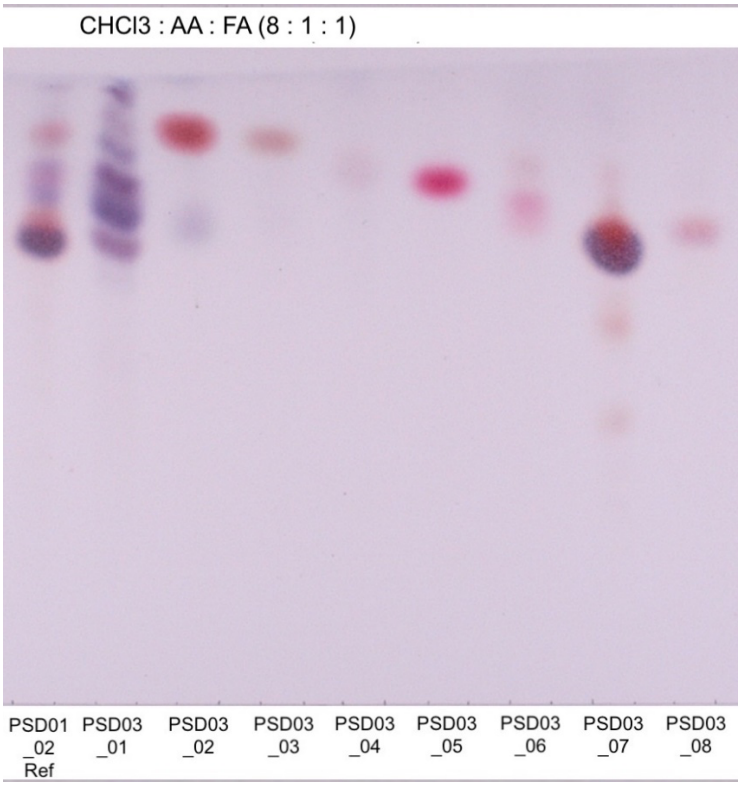

Figure 15: Collective-TLC analysis of HPCCC fractions PSD03_01 - PSD03_08; Detection in VIS after using spraying reagent vanillin/sulphuric acid

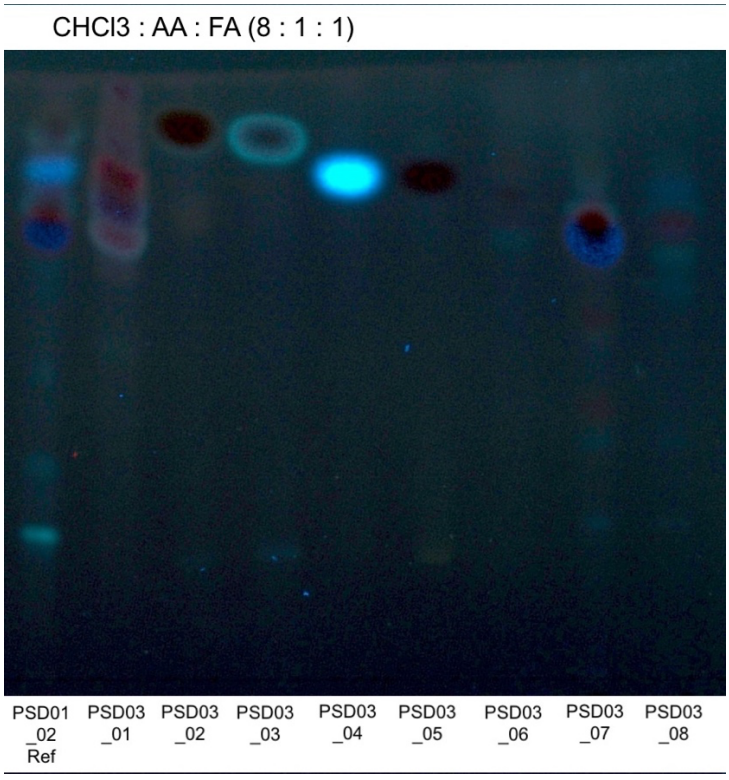

Figure 16: Collective-TLC analysis of HPCCC fractions PSD03_01 - PSD03_08; Detection at UV366 nm

4.1.5.2 UPLC of PSD03_01 to PSD03_08

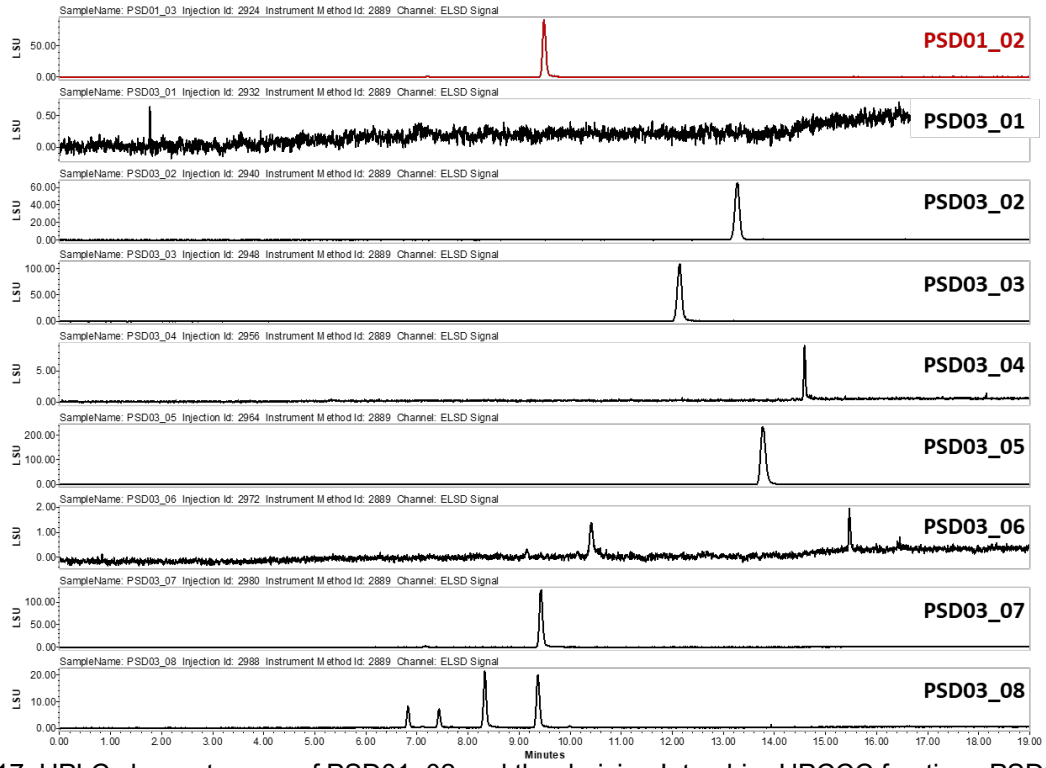

Figure 17: UPLC chromatogram of PSD01_02 and the deriving Interchim-HPCCC fractions PSD03_01 - PSD03_08. (ELSD)

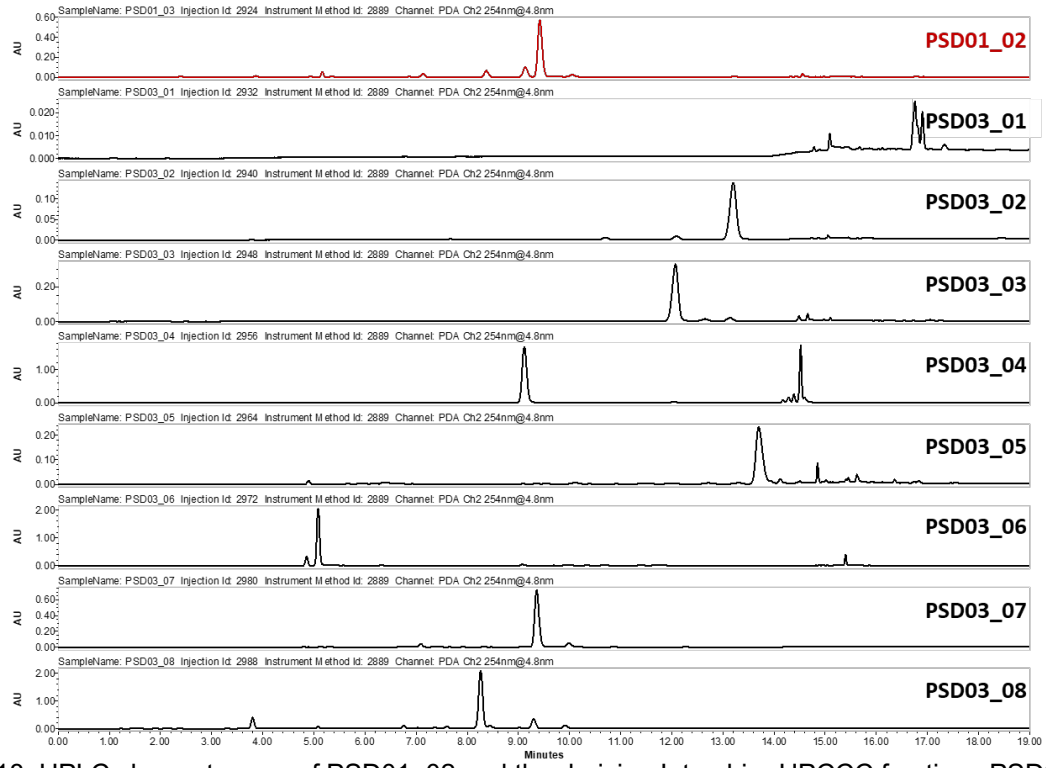

Figure 18: UPLC chromatogram of PSD01_02 and the deriving Interchim-HPCCC fractions PSD03_01 - PSD03_08. (PDA 254 nm)

4.1.5.3 Survival Assay of PSD01_01, PSD01_02 and the generated Interchim-HPCCC fractions PSD02_01 – PSD02_03 and PSD03_01 – PSD03_08

The bioactivity guided fractionation procedure was continued with the obtained Interchim-HPCCC fractions from PSD01_01 and PSD01_02. All sub-fractions of PSD01_01, i.e. PSD02_01 – PSD02_03 were able to increase the nematodes's DT_{50} value by 20.9% ($p < 0.05$), 16.2% (n.s.) and 24.5% ($p < 0.01$), respectively. PSD01_02 on the other hand showed in the previous experiments detrimental effects on the nematodes DT_{50} value (Figure 11 and Table 3). Within this screening, the lifespan shortening effect of PSD01_02 was confirmed (DT_{50} reduction of 9.6%). Strikingly, only one sub-fraction of PSD01_02 drastically decreasesd the nematodes's mean survival rate with a DT_{50} reduction of 28.2% ($p < 0.01$), namely PSD03_05. The other sub-fractions had no significant lifespan prolonging/shortening effect, i.e. PSD03_02, PSD03_06, PSD03_07 and PSD03_08, whereas PSD03_01, PSD03_03 and PSD03_04 significantly led to a DT_{50} extension of 19.8% ($p < 0.05$), 31.7% ($p < 0.01$) and 25.1% ($p < 0.01$), respectively.

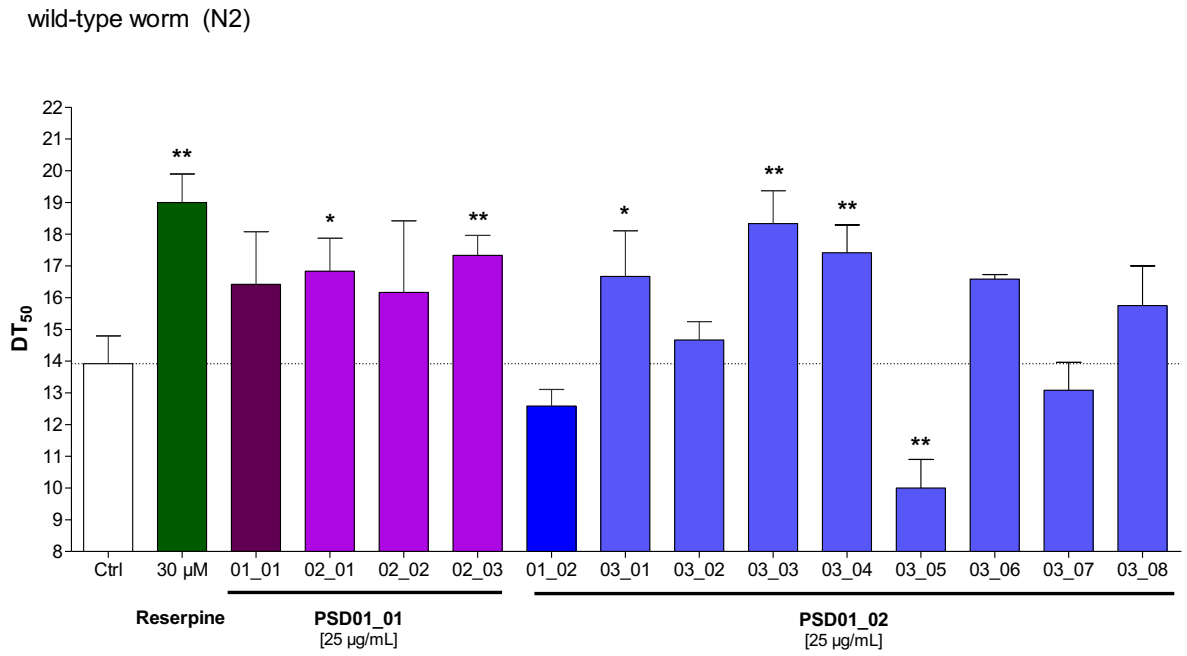

Figure 19: Results of a C. elegans Lifespan Assay with N2 wild-type worms; The puriFlash Interchim fraction PSD01_01 with the obtained HPCCC fractions PSD02_01 – PSD02_03,the puriFlash Interchim fraction PSD01_02 with the obtained HPCCC fractions PSD03_01 – PSD03_08 (all at 25 and 10 µg/mL), the vehicle control (DMSO 1%) and the positive control reserpine 30 µM were assayed for lifespan prolonging effects. Bars represent the mean DT_{50} ± SD of three parallel experiments. Significance was assessed by One-Way ANOVA with Dunnett's post-test (*p < 0.05; **p < 0.01).

Table 4 Survival analysis upon treatment with the Puriflash Interchim fractions PSD01_01 – PSD01_02 and the obtained Interchim-HPCCC fractions PSD02_01 – PSD02_03 and PSD03_01 – PSD03_08. One way ANOVA with Dunnett's post-test was used for statistical evaluation. *P*-value < 0.05 was considered as statistically significant.

Sample	*c*	Mean DT_{50} ± SD	DT_{50} extension (%)	*p*-value
Control	-	13.92 ± 0.88	-	-
Reserpine	30 µM	19.00 ± 0.90	36.49	***p* < 0.01**
PSD01_01	25 µg/mL	16.42 ± 1.67	17.96	*p* > 0.05
PSD02_01	25 µg/mL	16.83 ± 1.04	20.91	***p* < 0.05**
PSD02_02	25 µg/mL	16.17 ± 2.26	16.16	*p* > 0.05
PSD02_03	25 µg/mL	17.33 ± 0.63	24.50	***p* < 0.01**
PSD01_02	25 µg/mL	12.58 ± 0.52	-9.63	*p* > 0.05
PSD03_01	25 µg/mL	16.67 ± 1.44	19.76	***p* < 0.05**
PSD03_02	25 µg/mL	14.67 ± 0.58	5.39	*p* > 0.05
PSD03_03	25 µg/mL	18.33 ± 1.04	31.68	***p* < 0.01**
PSD03_04	25 µg/mL	17.42 ± 0.88	25.14	***p* < 0.01**
PSD03_05	25 µg/mL	10.00 ± 0 90	-28.16	***p* < 0.01**
PSD03_06	25 µg/mL	16.58 ± 0.14	19.11	*p* > 0.05
PSD03_07	25 µg/mL	13.08 ± 0.88	-6.03	*p* > 0.05
PSD03_08	25 µg/mL	15.75 ± 1.25	13.15	*p* > 0.05

4.1.6 Isolation and Characterization of Distinct Bioactive Fractions generated from PtesanXDM

Extraction from the heartwood of *P. santalinus* was performed as part of a previous thesis, and 13 fractions (PS01_01 - PS01_13) were obtained from the generated crude extract PtesanXDM_LS using HPCCC (Thrakl, 2019). During this present work, two of the 13 fractions, namely PS01_04 and PS01_07 were further purified by sephadex CC and the isolates were analyzed by 2D NMR (following Chapters). An overview of the workflow is shown in Figure 20. Furthermore, a previous *C. elegans* lifespan assay showed that the 13 HPCCC fractions had an interesting effect on the nematodes' lifespan. Therefore, these fractions were investigated in further lifespan and juglone-induced stress resistance assays on wild-type worms (N2), *daf-16* loss-of-function worms (CF1038) and *skn-1* loss-of-function worms (EU1) (Chapter 4.3).

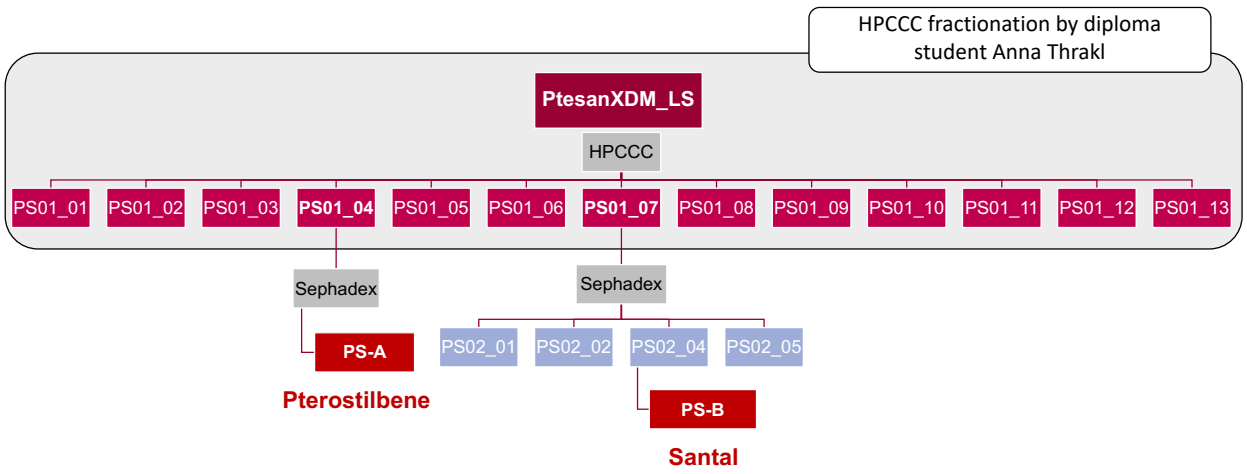

Figure 20: Workflow of the already produced HPCCC fractions PS01_01 - PS01_13

4.1.6.1 Sephadex Column Chromatography of PS01_04 and PS01_07

Based on the information obtained by thin layer chromatography and a dereplication performed earlier, we decided to further purify fractions PS01_04 and PS01_07 by sephadex CC. Sephadex CC separates molecules according to their size, with larger molecules eluting more rapidly from the column compared to smaller molecules. 22.1 mg of PS01_04 and 42.1 mg of PS01_07 were each dissolved in approximately 2 ml of MeOH and applied to the sephadex column. Methanol was used as the mobile phase for both experiments. Fractions were collected using a fraction collector, with 147 fractions collected from sample PS01_04 and 111 fractions collected from sample PS01_07. The separations were monitored by TLC (chromatogram not shown), similar fractions combined, and the isolates were further identified by 2D-NMR analysis and LC-MS experiments. Detailed parameters of the sephadex CC are described in Chapter 6.1.4.6.

4.1.6.2 Identification and Structure Elucidation of Isolates via 2D NMR

4.1.6.2.1 PS-A

Fraction PS01_04 consisted of one main compound, referred to as PS-A. The spectral data of the pure compound are given in Chapter 6.1.5. For NMR analysis, approximately 1 mg of the pure compound was dissolved in MeOH-d4. PS-A was identified as pterostilbene (Table 5). Pterostilbene, also 3,5-dimethoxy-4'-hydroxystilbene, is a known substance which has already been reported several times as a constituent from the heartwood of *P. santalinus* (Obrador, et al., 2021). It has antioxidant, anti-inflammatory, antibacterial and antitumor properties among others. It has also been reported to possess beneficial effects as an anti-aging compound and has potential for the prevention and treatment of age-related diseases by modulating different mechanisms (Li, Li, & Lin, 2018).

Table 5: PS-A

Fraction PS01_04				
Pure Compound	CAS Number	Substance Name	Molecular Weight	Structure
PS-A	537-42-8	pterostilbene	256.30	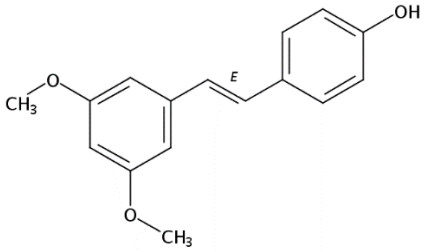

4.1.6.2.2 PS-B

Fraction PS01_07 was separated into fractions PS02_01, PS02_02, PS02_04 and PS02_05 by sephadex CC. PS02_04 (= PS-B) was identified as the isoflavonoid santal (Table 6). The spectral data of the pure compound are given in Chapter 6.1.5. The remaining fractions were either not pure enough or the amount of compounds was not sufficient for NMR analysis. Santal is a flavonoid that has already been isolated from the heartwood of *P. santalinus* (Krishnaveni & Srinivasa Rao, 2000). More detailed information about the substance has not yet been described in literature.

Table 6: PS-B

Fraction PS01_07				
Pure Compound	CAS Number	Substance Name	Molecular Weight	Structure
PS-B	529-60-2	santal	300.26	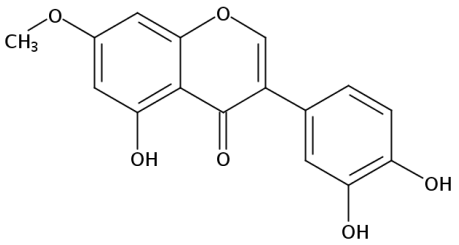

4.2 Phenotypic Screening of Selected Samples Affecting the Health Span of *Caenorhabditis elegans*

4.2.1 Lifespan Assay

4.2.1.1 Life Span Assay with wild-type worms (N2) and *daf-16* loss-of-function worms (CF1038)

In this lifespan assay, the positive control reserpine at a concentration of 30 µM, the large-scale extract PtesanXDM_LS and the HPCCC fractions PS01_01 - PS01_13 (all at 25 µg/mL) were tested on wild-type worms (N2) and *daf-16* loss-of-function worms (CF1038).

The results are as follows: In the wild-type worms, reserpine and PtesanXDM_LS showed a significant increase in nematode lifespan compared to vehicle control DMSO 1% (DT_{50} extension of 28.4% ($p < 0.01$) and 18.6% ($p < 0.05$). Moreover, four of the thirteen fractions tested, namely PS01_01, PS01_05, PS01_08 and PS01_13 caused a significant increase by 25.1% ($p < 0.01$), 17.6% ($p < 0.05$), 16.7% ($p < 0.05$) and 19.0% ($p < 0.05$). One of the fractions tested, namely PS01_04 caused a significant decrease of 33.5% ($p < 0.01$) of the mean survival rate compared to the vehicle control (Figure 21 and Table 7).

In comparison, the lifespan prolonging effects previously shown in the N2 wild-type worms had disappeared in the *daf-16* mutants, and compared with the vehicle control, neither the positive control reserpine, PtesanXDM_LS, nor the HPCCC fractions, showed any significant reduction or increase in worm lifespan. This suggests that the lifespan prolonging effect of all fractions and also of the positive control reserpine is dependent on *daf-16*. Only the life-shortening effect of PS01_04 is independent of *daf-16*, as in both worm strains the mean survival rate is very similar and ranges between 11 - 12 days.

4.2.1.1.1 LSA_N2_PS01_A/B/C vs LSA_CF1038_PS01_A/B/C

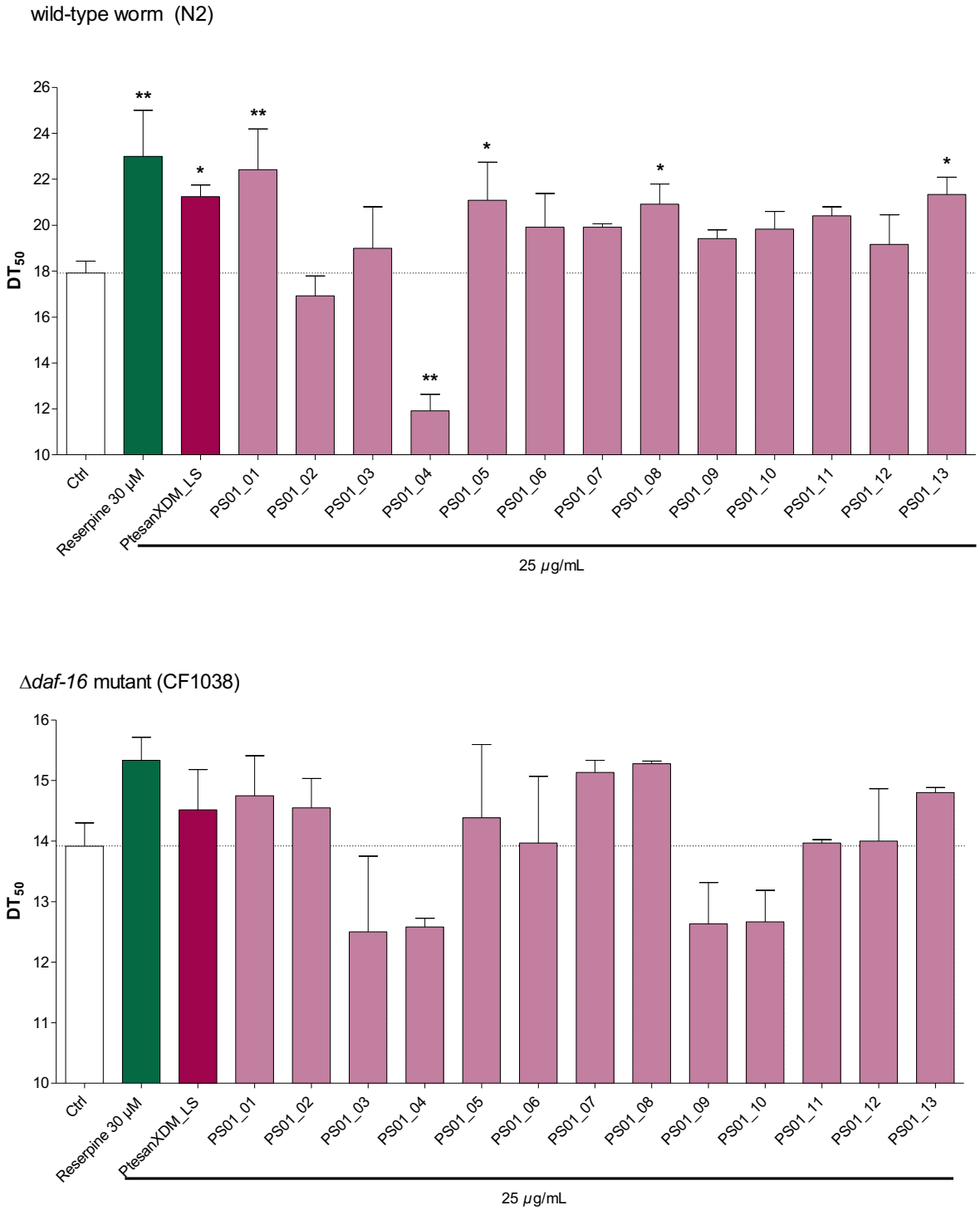

Figure 21: Results of a *C. elegans* Lifespan Assay with (i) N2 wild-type worms and (ii) daf-16 loss of function mutants CF1038; HPCCC fractions PS01_01 – PS01_13, the crude extract PtesanXDM (all at 25 µg/mL), the vehicle control (DMSO 1%) and the positive control reserpine 30 µM were assayed for lifespan prolonging effects. Bars represent the mean DT_{50} ± SD of three parallel experiments.Significance was assessed by One-Way ANOVA with Dunnett's post-test (*p < 0.05; **p < 0.01).

Table 7: Survival analysis upon treatment with HPCCC fractions PS01_01 – PS01_13 in (i) N2 wild-type worms and (ii) daf-16 loss of function mutants CF1038; One way ANOVA with Dunnett's post-test was used for statistical evaluation. *P*-value < 0.05 was considered as statistically significant.

(N2)	**Sample**	***c***	**Mean DT_{50} ± SD**	**DT_{50} extension (%)**	***p*-value**
	Control	-	17.92 ± 0.52	-	-
	Reserpine	30 µM	23.00 ± 2.00	28.35	$p < 0.01$
	PtesanXDM_LS	25 µg/mL	21.25 ± 0.50	18.58	$p < 0.05$
	PS01_01	25 µg/mL	22.42 ± 1.77	25.11	$p < 0.01$
	PS01_02	25 µg/mL	16.92 ± 0.88	-5.58	$p > 0.05$
	PS01_03	25 µg/mL	19.00 ± 1.80	6.03	$p > 0.05$
	PS01_04	25 µg/mL	11.92 ± 0.72	-33.48	$p < 0.01$
	PS01_05	25 µg/mL	21.08 ± 1.67	17.63	$p < 0.05$
	PS01_06	25 µg/mL	19.92 ± 1.47	11.16	$p > 0.05$
	PS01_07	25 µg/mL	19.92 ± 0.14	11.16	$p > 0.05$
	PS01_08	25 µg/mL	20.92 ± 0.88	16.74	$p < 0.05$
	PS01_09	25 µg/mL	19.42 ± 0.38	8.37	$p > 0.05$
	PS01_10	25 µg/mL	19.83 ± 0.76	10.66	$p > 0.05$
	PS01_11	25 µg/mL	20.42 ± 0.38	13.95	$p > 0.05$
	PS01_12	25 µg/mL	19.17 ± 1.28	6.98	$p > 0.05$
	PS01_13	25 µg/mL	21.33 ± 0.76	19.03	$p < 0.05$
Δ*daf-16* mutant (CF1038)	Sample	*c*	Mean DT_{50} ± SD	DT_{50} extension (%)	*p*-value
	Control	-	13.92 ± 0.38	-	-
	Reserpine	30 µM	15.33 ± 0.38	13.56	$p > 0.05$
	PtesanXDM_LS	25 µg/mL	14.52 ± 0.66	7.56	$p > 0.05$
	PS01_01	25 µg/mL	14.75 ± 0.66	9.26	$p > 0.05$
	PS01_02	25 µg/mL	14.55 ± 0.48	7.78	$p > 0.05$
	PS01_03	25 µg/mL	12.50 ± 1.25	-7.41	$p > 0.05$
	PS01_04	25 µg/mL	12.58 ± 0.14	-6.81	$p > 0.05$
	PS01_05	25 µg/mL	14.38 ± 1.21	6.52	$p > 0.05$
	PS01_06	25 µg/mL	13.97 ± 1.10	3.48	$p > 0.05$
	PS01_07	25 µg/mL	15.13 ± 0.20	12.07	$p > 0.05$
	PS01_08	25 µg/mL	15.28 ± 0.05	13.19	$p > 0.05$
	PS01_09	25 µg/mL	12.63 ± 0.68	-6.44	$p > 0.05$
	PS01_10	25 µg/mL	12.67 ± 0.52	-6.15	$p > 0.05$
	PS01_11	25 µg/mL	13.97 ± 0.06	3.48	$p > 0.05$
	PS01_12	25 µg/mL	14.00 ± 0.87	3.70	$p > 0.05$
	PS01_13	25 µg/mL	14.80 ± 0.09	9.63	$p > 0.05$

4.2.2 Stress Resistance Assay

4.2.2.1 Stress Resistance Assay with N2 worms (wild-type)

4.2.2.1.1 SRA_N2_03_A/B/C

A survival assay under juglone-induced oxidative stress was performed with the crude extract PtesanXDM. Briefly, synchronized, adult worms were pre-treated for 5 days with the respective samples at 25 °C. 48 h after juglone exposure (at a final concentration of 80 µM) the survival of the worms was monitored. The results of the juglone-induced stress resistance assay using the wild-type worms N2 are as follows: the positive control epigallocatechin gallate (EGCG; tested at 100 µM) as well as the crude extract PtesanXDM_LS (at 100 and 25 µg/mL) showed a significant increase of the mean survival rate when compared to the vehicle control DMSO 1% (Figure 22 and Table 8).

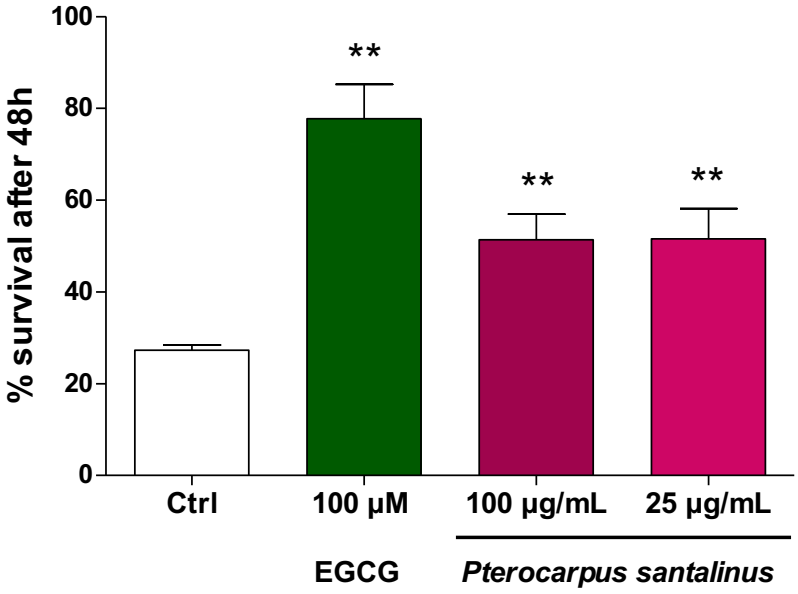

Figure 22: Results of a *C. elegans* Stress Resistance Assay with N2 wild-type worms; the crude extract PtesanXDM_LS (100 and 25 µg/mL), the vehicle control (DMSO 1%) and the positive control epigallocatechin gallate (EGCG) 100 µM were assayed for oxidative stress resistance. Before exposure to the pro-oxidative compound juglone (80 µM), worms were pre-treated for 5 days with the extract and fractions, respectively. Bars represent the mean survival rate (%) ± SD of three parallel experiments. Significance was assessed by One-Way ANOVA with Dunnett's post-test (*$p < 0.05$; **$p < 0.01$).

Table 8: Juglone-incuded stress-resistance analysis upon treatment with PtesanXDM_LS in wild-type worms. One way ANOVA with Dunnett's post-test was used for statistical evaluation. *P*-value < 0.05 was considered as statistically significant.

Sample	*c*	Mean % survival ± SD	*p*-value
Control	-	27.27 ± 1.16	-
EGCG	30 µM	77.73 ± 7.57	$p < 0.01$
PtesanXDM_LS	100 µg/mL	51.36 ± 5.60	$p < 0.01$
	25 µg/mL	51.55 ± 6.59	$p < 0.01$

4.2.2.1.2 SRA_N2_PS01_A/B/C

The 13 HPCCC fractions were investigated in the juglone-induced stress resistance assay using the wild-type worms N2. Synchronized, adult worms were pre-treated for 5 days with the respective samples. 48 h after juglone exposure at 80 µM the survival of the worms was monitored. The mean survival rate of the worms was significantly higher for the positive control EGCG (at 100 µM; 76.9 ± 14.1%), the crude extract PtesanXDM_LS (62.3 ± 14.8%) and for two fractions, namely PS01_06 (69.0 ± 10.6%) and PS01_07 (60.7 ± 12.9%; all at 25 µg/mL), when compared to the vehicle control (21.3 ± 5.8%; Figure 23 and Table 9).

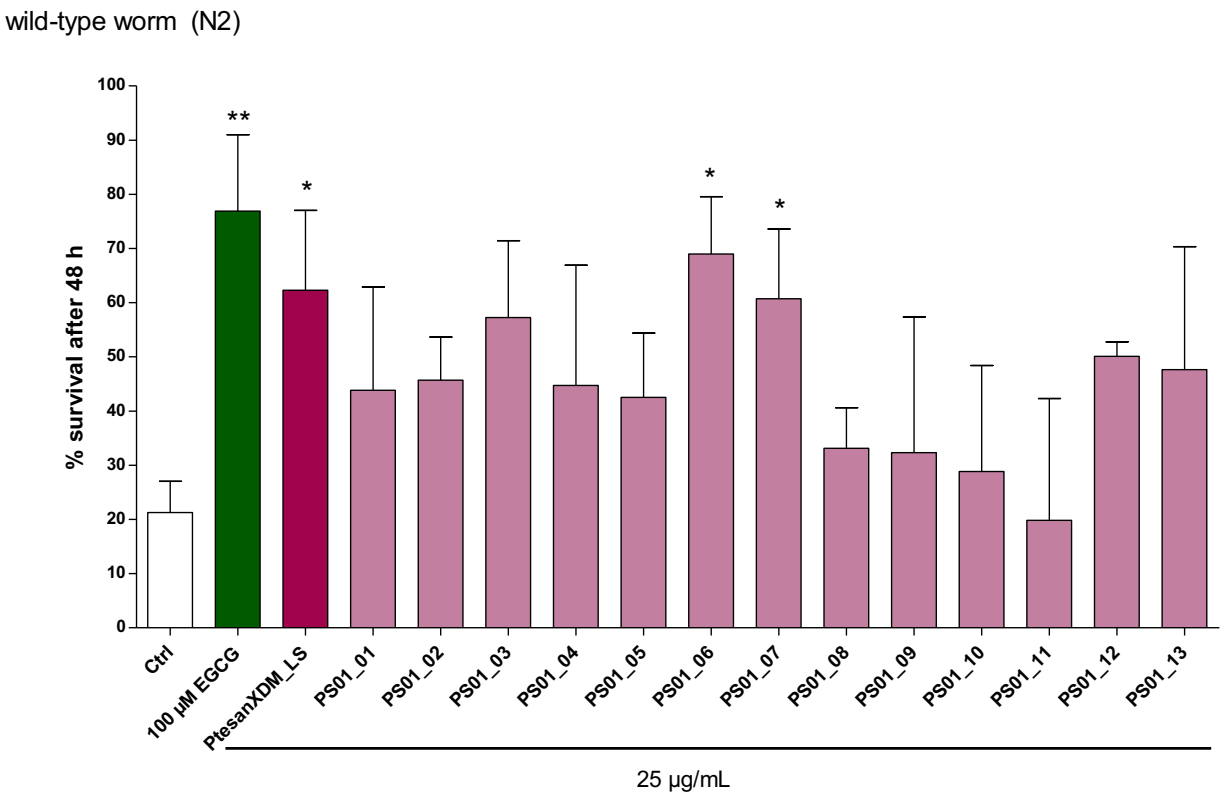

Figure 23: Results of a *C. elegans* Stress Resistance Assay with N2 wild-type worms; the crude extract PtesanXDM_LS, the HPCCC fractions PS01_01 – PS01_13 (all at 25 µg/mL), the vehicle control (DMSO 1%) and the positive control epigallocatechin gallate (EGCG) 100 µM were assayed for oxidative stress resistance. Before exposure to the pro-oxidative compound juglone (80 µM), worms were pre-treated for 5 days with the extract and fractions, respectively. Bars represent the mean survival rate (%) ± SD of three parallel experiments. Significance was assessed by One-Way ANOVA with Dunnett's post-test (*$p < 0.05$; **$p < 0.01$).

Table 9: Juglone-incuded stress-resistance analysis upon treatment with PtesanXDM_LS and HPCCC fractions PS01_01 – PS01_13 in wild-type worms. One way ANOVA with Dunnett's post-test was used for statistical evaluation. P-value < 0.05 was considered as statistically significant.

Sample	*c*	Mean % survival ± SD	*p*-value
Control	-	21.28 ± 5.77	-
EGCG	100 µM	76.92 ± 14.07	$p < 0.01$
PtesanXDM_LS	25 µg/mL	62.29 ± 14.76	$p < 0.05$
PS01_01	25 µg/mL	43.85 ± 19.04	$p > 0.05$
PS01_02	25 µg/mL	45.69 ± 7.89	$p > 0.05$
PS01_03	25 µg/mL	57.27 ± 14.16	$p > 0.05$
PS01_04	25 µg/mL	44.73 ± 22.17	$p > 0.05$
PS01_05	25 µg/mL	42.53 ± 11.87	$p > 0.05$
PS01_06	25 µg/mL	68.97 ± 10.59	$p < 0.05$
PS01_07	25 µg/mL	60.72 ± 12.88	$p < 0.05$
PS01_08	25 µg/mL	33.12 ± 7.50	$p > 0.05$
PS01_09	25 µg/mL	32.33 ± 25.06	$p > 0.05$
PS01_10	25 µg/mL	28.86 ± 19.55	$p > 0.05$
PS01_11	25 µg/mL	19.84 ± 22.46	$p > 0.05$
PS01_12	25 µg/mL	50.09 ± 2.71	$p > 0.05$
PS01_13	25 µg/mL	47.66 ± 22.69	$p > 0.05$

4.2.2.2 Stress Resistance Assay with *daf-16* loss-of-function worms (CF1038)

4.2.2.2.1 SRA_CF1038_03_A/B/C

The stress resistance assay with *daf-16* loss of function mutants was performed as described before and provided interesting results: Similar as in the screening with the wild-type worms (Chapter 4.3.2.1.1, Figure 22), the positive control EGCG at 100 µM was able to significantly increase the survival rate of the worm when compared to the vehicle control (Figure 24 and Table 10). In contrast, the worms pre-treated with the crude extract PtesanXDM (at 100 and 25 µg/mL) showed no (significant) differences when compared to the vehicle control. This indicates that the lifespan prolonging effect observed in the wild-type worms is dependent on the presence of the transcription factor *daf-16*.

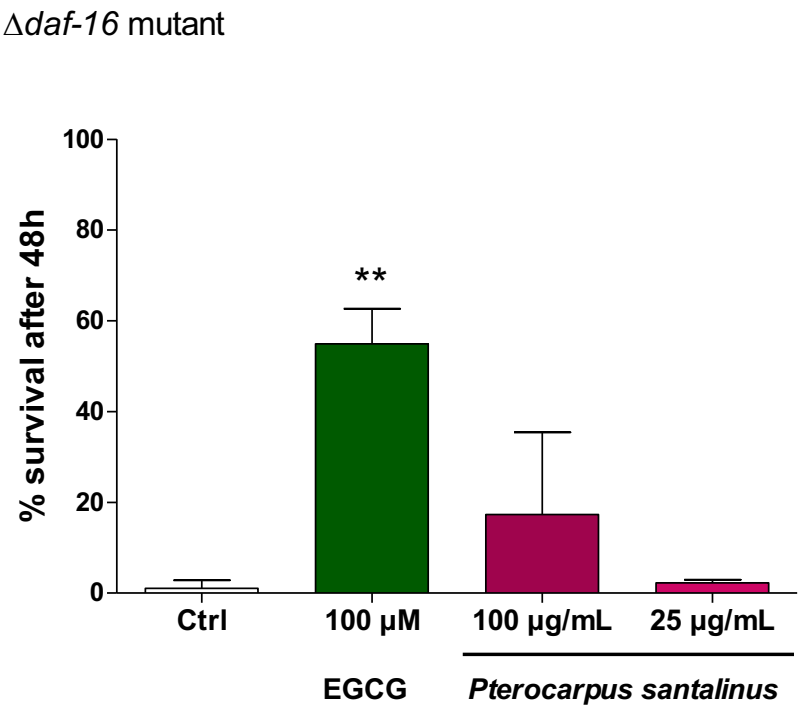

Figure 24: Results of a *C. elegans* Stress Resistance Assay with *daf-16* loss-of-function mutants (CF1038); the crude extract PtesanXDM (100 and and 25 µg/mL), the vehicle control (DMSO 1%) and the positive control epigallocatechin gallate 100 µM were assayed for oxidative stress resistance. Before exposure to the pro-oxidative compound juglone (80 µM), worms were pre-treated for 5 days with the extract and fractions, respectively. Bars represent the mean survival rate (%) ± SD of three parallel experiments. Significance was assessed by One-Way ANOVA with Dunnett's post-test (*p < 0.05; **p < 0.01).

Table 10: Juglone-incuded stress-resistance analysis upon treatment with PtesanXDM_LS *in daf-16* loss-of-function mutants (CF1038). One way ANOVA with Dunnett's post-test was used for statistical evaluation. P-value < 0.05 was considered as statistically significant.

Sample	*c*	Mean % survival ± SD	*p*-value
Control	-	1.04 ± 1.81	-
EGCG	100 µM	54.93 ± 7.74	$p < 0.01$
PtesanXDM_LS	100 µg/mL	17.32 ± 18.09	$p > 0.05$
	25 µg/mL	2.24 ± 0.68	$p > 0.05$

4.2.2.2.2 SRA_CF1038_PS01_A/B/C

The 13 HPCCC fractions were investigated in the juglone-induced stress resistance assay using the mutant worms CF1038. Unfortunately, the experiment failed, as shown in Figure 25. From the vehicle control it can be seen that most of the worms were still not dead after 96 h of juglone-exposure. Most of the worms were expected to be dead after 48h as described before. Therefore, this experiment must be repeated in future experiments.

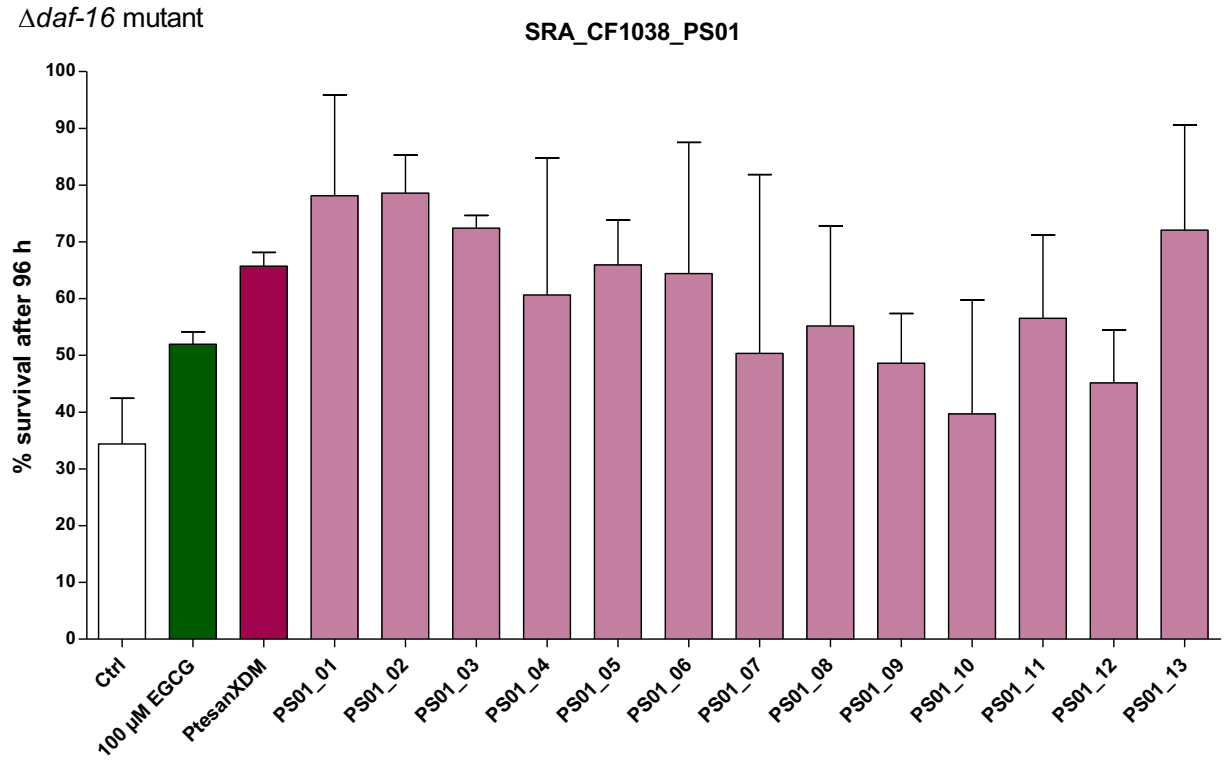

Figure 25: Results of a *C. elegans* Stress Resistance Assay with *daf-16* loss-of-function mutants (CF1038); the crude extract PtesanXDM, the HPCCC fractions PS01_01 – PS01_13 (all at 25 µg/mL), the vehicle control (DMSO 1%) and the positive control epigallocatechin gallate (EGCG) 100 µM were assayed for oxidative stress resistance. Before exposure to the pro-oxidative compound juglone (80 µM), worms were pre-treated for 5 days with the extract and fractions, respectively. Bars represent the mean survival rate (%) ± SD of three parallel experiments. Significance was assessed by One-Way ANOVA with Dunnett's post-test (*$p < 0.05$; **$p < 0.01$).

4.2.2.3 Stress Resistance Assay with *skn-1* loss-of-function worms (EU1)

4.2.2.3.1 SRA_EU1_A/B/C

The stress resistance assay with *skn-1* loss of function mutants was performed as described before and provided interesting results: worms treated with the positive control EGCG at 100 µM (73.2 ± 13.1%), PtesanXDM at 100 µg/mL (79.2 ± 18.2%) and 25 µg/mL (84.8 ± 6.3%) resulted in significantly higher survival rates when compared to the vehicle control (27.7 ± 15.4%) (Figure 26 and Table 11). This suggests that the lifespan prolonging effect of PtesanXDM observed in the wild-type worms is not dependent on the transcription factor *skn-1.*

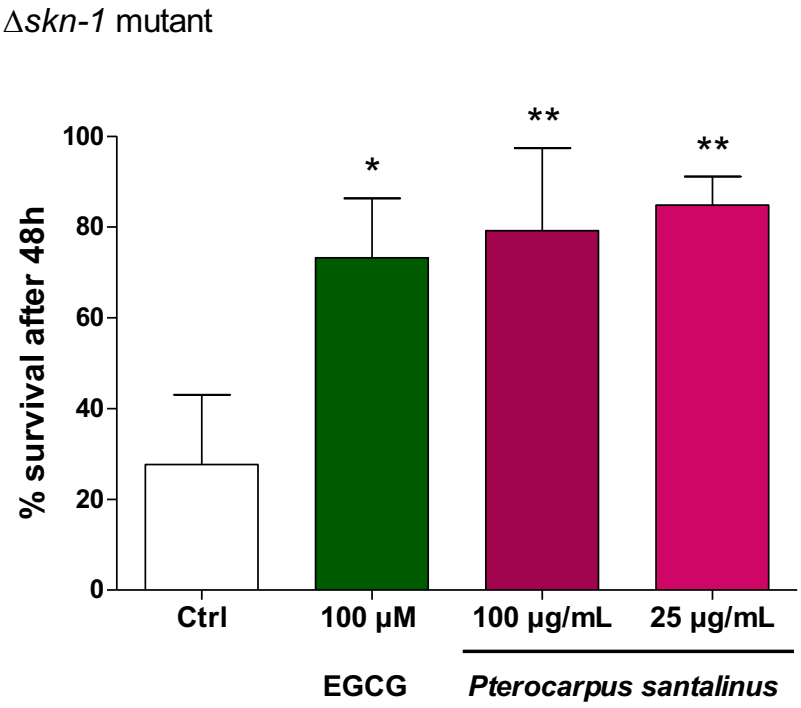

Figure 26: Results of a *C. elegans* Stress Resistance Assay with skn-1 loss-of-function mutants (EU1); the crude extract PtesanXDM (100 and and 25 µg/mL), the vehicle control (DMSO 1%) and the positive control epigallocatechin gallate (EGCG) 100 µM were assayed for oxidative stress resistance. Before exposure to the pro-oxidative compound juglone (80 µM), worms were pre-treated for 5 days with the extract and fractions, respectively. Bars represent the mean survival rate (%) ± SD of three parallel experiments. Significance was assessed by One-Way ANOVA with Dunnett's post-test (*p < 0.05; **p < 0.01).

Table 11 Juglone-incuded stress-resistance analysis upon treatment with PtesanXDM_LS in skn-1 loss-of-function mutants (EU1). One way ANOVA with Dunnett's post-test was used for statistical evaluation. P-value < 0.05 was considered as statistically significant.

Sample	*c*	Mean % survival ± SD	*p*-value
Control	-	27.67 ± 15.37	-
EGCG	100 µM	73.19 ± 13.12	$p < 0.05$
PtesanXDM_LS	100 µg/mL	79.17 ± 18.17	$p < 0.01$
	25 µg/mL	84.82 ± 6.32	$p < 0.01$

5 CONCLUSION

Preliminary experiments performed with the MeOH-DCM heartwood extract of *P. santalinus* showed promising lifespan prolonging effects in a *C. elegans* lifespan assay. Based on these observations, this diploma thesis aims to isolate and characterize bioactive constituents that affect the healthspan of the nematode *C. elegans*. Therefore, two of the existing HPCCC fractions PS01_01 - PS01_13 were further purified using Sephadex CC. In previous experiments the fraction PS01_04 significantly decreased the DT_{50} of treated worms in comparison to untreated worms by 33.5%. The purification with Sephadex CC resulted in the pure compound PS-A. 1D- and 2D-NMR experiments identified the isolated compound as the resveratrol derivative pterostilbene. From fraction PS01_07, which was able to increase the DT_{50} value by 11.2%, the pure compound PS-B was isolated and identified as the isoflavonoid santal. Both compounds have already been described for *P. santalinus* before (Obrador, et al., 2021; Krishnaveni & Srinivasa Rao, 2000). In addition, pterostilbene has already been identified to possess detrimental effects on worm survival: at 100 µM the stilbene compound was able to reduce de survival rate of adult worms by 28% (Wilson, Rimando, & Wolkow, 2008). Since PS01_04 consists of mainly pterostilbene and was tested at 25 µg/mL (which correlates to ~ 97 µM) our data is in line with the previously reported effects on *C. elegans*. In contrast, this is the first time that the isoflavonoid santal was reported to possess anti-aging effects *in vivo*.

Unfortunately, the crude extract PtesanXDM contains a high quantity of persistent staining pigments. In order to enhance the isolation efficiency of (unknown) secondary metabolites apart from pigments with potential bioactivities, a liquid-liquid separation of the crude extract PtesanXDM was performed. A separation-protocol was generated using 50% aqueous MeOH and DCM. A total of ~85 g of PtesanXDM were successfully partitioned in a separation funnel in the pigment-depleted and concurrently secondary-metabolite-enriched fraction PtesanXDM_DCM and the pigment-enriched fraction PtesanXDM_MW. A *C. elegans* lifespan assay revealed significant lifespan-prolonging properties for the pigment-depleted fraction PtesanXDM_DCM (able to extend the DT_{50} significantly by 18.9% when tested at 10 µg/mL). Hence, PtesanXDM, which seemed to contain the responsible bioactive secondary metabolites, was further investigated. ~10 g of PtesanXDM_DCM was separated into four fractions, i.e. PSD01_01 - PSD01_04, using the Purifash Interchim in a large-scale, normal phase manner. The obtained fractions were analyzed in the *C. elegans* lifespan assay at 25 and 10 µg/mL as described before. At 10 µg/mL PSD01_01 resulted in a DT_{50} extension of 19.4%, whereas at the higher

concentration of 25 µg/mL the DT_{50} was reduced by ~ 8% (both n.s.). PSD01_02 showed hardly any effect at 10 µg/mL (DT_{50} extension of 4.0%) whereas at 25 µg/mL the fraction significantly decreased the DT_{50} value by 31.6% ($p < 0.05$). PSD01_03 extended the mean survival rate of the nematodes by 36.9% and 36.2% (at 25 and 10 µg/mL; both $p < 0.05$) when compared to the vehicle control. The TLC pattern PSD01_04 looks similar to the pigment-enriched fraction PtesanXDM_MW and showed hardly any effect on the lifespan of *C. elegans.* Within the scope of this diploma thesis, PSD01_01 and PSD01_02 were further investigated via InterHPCCC. Fraction PSD01_01 was separated into three sub-fractions (i.e. PSD02_01 - PSD02_03) and fraction PSD01_02 was further separated into eight sub-fractions (i.e. PSD03_01 - PSD03_08). Again, a lifespan assay with wild-type worms was performed. PSD02_01 - PSD02_03 increased the DT_{50} value of nematodes by 20.9% ($p < 0.05$), 16.2% (n.s.) and 24.5% ($p < 0.01$), respectively. Sub-fractions PSD03_02, PSD03_06, PSD03_07, and PSD03_08 had no significant life-extending/shortening effect on the worms, whereas the sub-fractions PSD03_01, PSD03_03, and PSD03_04 showed significant lifespan prolonging effect of 19.8% ($p < 0.05$), 31.7% ($p < 0.01$) and 25.1% ($p < 0.01$), respectively. In contrast, the sub-fraction PSD03_05 showed detrimental effects on the mean survival rate of nematodes with a DT_{50} reduction of 28.2% ($p < 0.01$). The observed nematotoxicity could be of interest for the disclosure of anti-helminthic compound(s) and remains a topic for further investigations.

The last part of this thesis was dedicated to the phenotypic screening with mutant worms, such as the *daf-16* loss-of-function mutant CF1038 and the *skn-1*-loss-of-function mutant EU1. The screening of the 13 HPCCC fractions PS01_01 - PS01_13 in a *C. elegans* lifespan assay and a juglone-induced stress resistance assay suggests that the lifespan prolonging effect PtesanXDM, which was observed in the wild-type worms N2, is dependent on the *daf-16* transcription factor and independent of the transcription factor *skn-1*. In order to confirm these findings, further assays with mutant worms have to be performed. For instance, nuclear localization of *daf-16/skn-1* can be visualized using a reporter strain where *daf-16/skn-1 is* fused to the green fluorescent protein (GFP).

6 MATERIALS AND METHODS

6.1 Isolation and Characterization of Bioactive Constituents from *Pterocarpus santalinus* affecting the Healthspan of *Caenorhabditis elegans*

6.1.1 Plant Material

The Large-Scale extract PtesanXDM used in this diploma thesis was obtained from the heartwood of *P. santalinus* generated in a previous work (Thrakl, 2019). Briefly, the ground heartwood of *P. santalinus* was purchased from Kottas Pharma GmbH (Batch no. P16301836; Eitnergasse 8, A-1230 Vienna) and extracted successively with dichloromethane (DCM) and methanol (MeOH).

6.1.2 Depletion of Pigments from the Large-Scale Extract PtesanXDM by Liquid-Liquid Separation

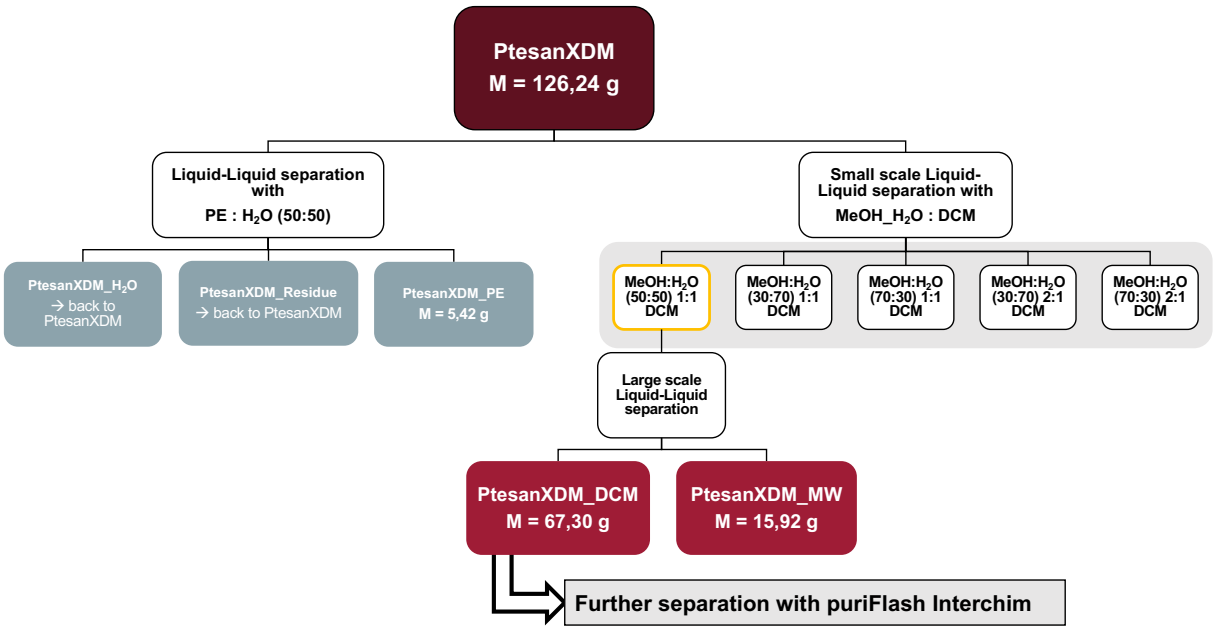

Figure 27: Flowchart of the Liquid-Liquid Separation steps of PtesanXDM

6.1.3 Labeling of Samples and Fractions

The extract and the generated fractions were labeled according to the following scheme: The first three letters of the genus and the first three letters of the species are merged (e.g., Ptesan for *Pterocarpus santalinus*). This is followed by the abbreviation for the

organ used (e.g., X stands for wood) and for the extraction solvent used (D stands for DCM and M for MeOH). HPCCC-fractionation without a previous fractionation step of the crude extract were designated PS01_XX, where PS stands for the species *Pterocarpus santalinus*, 01 for the first step of fractionation, and XX for the number of each fraction. These fractions were obtained by HPCCC as described in a previous diploma thesis (Thrakl, 2019). The puriFlash Interchim fractions generated in this diploma thesis were obtained after depletion of pigments (via liquid-liquid separation with DCM-MW) and were labeled according to the same principle, but additionally added with the letter D for DCM (e.g. PSD01_01). Further fractionation of PSD01_01 by HPCCC leads to the label PSD02_XX, where 02 stands for the second step of fractionation and XX again for the number of each fraction. Isolated substances were labeled with the initial letter of the genus, then the species, and then in letter order. (e.g. PS-A, PS-B).

6.1.4 Chromatographic Methods

6.1.4.1 Large-Scale Fractionation of PtesanXDM_DCM with puriFlash Interchim

Flash chromatography is a liquid chromatography technique that uses air pressure to push the mobile phase through the stationary phase column. This results in the ability to use very small silica gel particles and obtain a rapid and high-resolution separation (Roge, Firke, Kawade, Sarje, & Vadvalkar, 2011). The instrumentation used for this diploma thesis is the Interchim puriFlash® 4250 (Figure 28). The following tables show the conditions used for the analytical as well as preparative methods. For all experiments a photodiode array Detector (PDA) at a wavelength of 210 nm and a wavelength scan of 200 - 600 nm, and an evaporative light scattering detector (ELSD) were used as detectors.

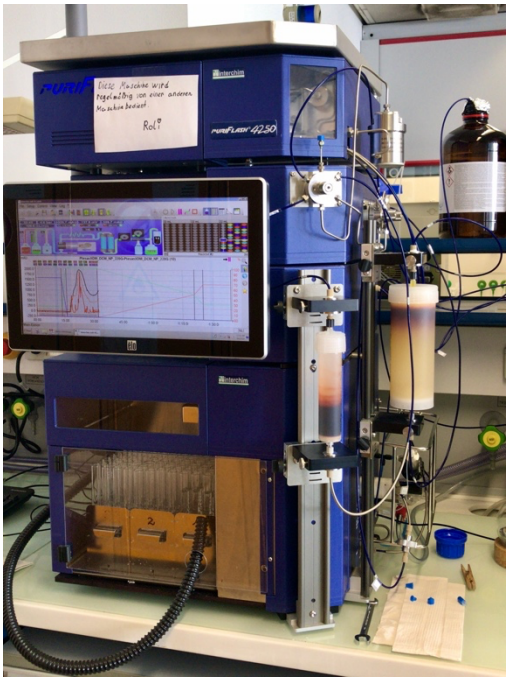

Figure 28: Interchim puriFlash ® 4250 during fraction collection

Table 12: Separation of PtesanXDM_DCM by analytical puriFlash

Method Name	PuriFlash Column	flow rate [mL/min]	mobile phase
PtesanXDM_DCM_RP_ACN	15 C18 HQ 6G	5	ACN + H_20
PtesanXDM_DCM_RP_MeOH	15 C18 HQ 6G	5	MeOH + H_20
PtesanXDM_DCM_NP_4G	15 SILICA HP 4G	5	MeOH + DCM + PE
PtesanXDM_DCM_NP_4G_2	15 SILICA HP 4G	5	MeOH + DCM + PE

Table 13: Separation of PtesanXDM_DCM by preparative puriFlash

Method: PtesanXDM_DCM_NP_220G			
column	**mode**	**flow rate**	**applied amount**
Puriflash column 25 Silica HC 200 G	Normal phase	100 mL/min	10.206 g
Time (h)	**% A (MeOH)**	**% B (DCM)**	**% C (PE)**
00:00:00	0	20	80
00:13:27	0	20	80
00:16:08	0	100	0
00:32:16	0	100	0
01:20:41	50	50	0
01:20:44	70	30	0
01:34:11	70	30	0

Table 14: Combined Fractions and Fraction yields of PSD01_01 – PSD01_04 after puriFlash Interchim fractionation

Fraction Name	Combined Fractions	Round bottom flask Weight [g]	Yield [g]
PSD01_01	1 - 140	168.65	1.27
PSD01_02	141 - 208	169.14	0.84
PSD01_03	209 - 261	170.61	5.13
PSD01_04	262 - 442	169.12	0.99

6.1.4.2 High-Performance Counter-Current Chromatography of PSD01_01

Table 15: HEMWat Systems Screening for PSD01_01

HEMWat No.	*n*-hex	EtOAc	MeOH	H_2O
17	1	1	1	1
19	3	2	3	2
21	5	2	5	2
23	4	1	4	1
25	6	1	6	1

Table 16: Flash-HPCCC parameters for the fractionation of PSD01_01

instrument	mode	column	flow Rate [ml/min]	inj. volume [ml]	rpm	pressure (bar)
Dynamic Extractions Spectrum	Normal - Phase	Semi - Preparative	6 - 10	10	200 - 1600	3-4

Time [min]	rpm	Flow Rate [mL/min]	% A [s.p. 23]	% B [m.p. 23]
00:00	200	10	100	0
30:00	200	10	100	0
32:00	200	6	100	0
32:03	1600	6	0	100
05:30:00	1600	6	0	100

Table 17: final fraction yields after Interchim-HPCCC fractionation of PSD01_01

Fraction Name	Vial Weight [g]	Fraction Yield [mg]
PSD02_01	6.96793	35.48
PSD02_02	7.04315	235.89
PSD02_03	6.91756	66.49

6.1.4.3 High-Performance Counter-Current Chromatography of PSD01_02

Table 18: HEMWat Systems Screening for PSD01_02

HEMWat No.	*n*-hex	EtOAc	MeOH	H_2O
15	2	3	2	3
17	1	1	1	1
18	6	5	6	5
19	3	2	3	2
20	2	1	2	1
21	5	2	5	2
23	4	1	4	1

Table 19: Flash-HPCCC parameters for the fractionation of PSD01_02

instrument	**mode**	**column**	**flow Rate [ml/min]**	**inj. volume [ml]**	**rpm**	**pressure (bar)**
Dynamic Extractions Spectrum	Normal - Phase	Semi - Preparative	6 - 10	10	200 - 1600	3-4

Time [min]	**rpm**	**Flow Rate [mL/min]**	**% A [s.p. 23]**	**% B [m.p. 23]**	**% C [m.p. 19]**
00:00	200	10	100	0	0
30:00	200	10	100	0	0
32:00	200	6	100	0	0
32:03	1600	6	0	100	0
01:40:00	1600	6	0	100	0
03:40:00	1600	6	0	0	100

Table 20: Final fraction yields Interchim-HPCCC fractionation of PSD01_02

Fraction Name	Vial Weight [g]	Fraction Yield [mg]
PSD03_01	7.04363	31.05
PSD03_02	6.92949	10.38
PSD03_03	6.86543	0.80
PSD03_04	6.91118	4.56
PSD03_05	7.03292	2.07
PSD03_06	6.89644	2.97
PSD03_07	6.97396	166.11
PSD03_08	6.98293	8.22

6.1.4.4 TLC System

Stationary phase	TLC Silica gel 60 F_{254}
Mobile phase	$CHCl_3$: AA : FA (8 : 1 : 1)
Spraying reagent	Vanillin / H_2SO_4
Detection	UV_{254}, UV_{366}, VIS

6.1.4.5 Ultra-High Performance Liquid Chromatography

Table 21: Used UHPLC Method

Method: PtesanXDM_PDA_ELSD_col2						
instrument	**column**	**temp. [°C]**	**flow rate [mL/min]**	**inj vol [µl]**	**config.**	**det. wavel. [nm]**
UPLC Waters	TSS T3 100mm	40	0.250	5	PDA ELSD	210, 254, 190-400

time [min]	**mobile phase A [%] (H_2O)**	**mobile phase B [%] (ACN)**
0.00	70	30
0.50	70	30
2.00	55	45
3.50	50	50
12.00	45	55
12.10	2	98
16.00	2	98
16.10	70	30
17.00	70	30

6.1.4.6 Sephadex Column Chromatography of PS01_04 and PS01_07

Fractionation of PS01_04

Column No.	1
Stationary phase	Sephadex LH – 20 length: 1 m diameter: 1.5 cm
Mobile phase	MeOH
Amount of sample	22.08 mg
Fractions collected	147

Figure 29: Sephadex column during fraction collection

Fractionation of PS01_07

Column No.	1
Stationary phase	Sephadex LH – 20 length: 1 m diameter: 1.5 cm
Mobile phase	MeOH
Amount of sample	42.14 mg
Fractions collected	111

6.1.5 2D NMR Spectra of isolated compounds

Table 22 ^{1}H and ^{13}C NMR spectral data of PS-A

PS-A (Pterostilbene)					
δ H [ppm]	Protonen - anzahl	Multiplizität (J in Hz)	δ C [ppm]	δ C [ppm] aus HMBC	COSY
3.80	6	s	**55.72**	**162.49**	6.66 / 6.35
6.35	1	t (2.2 Hz)	**100.31**	**105.16, 162.49**	6.90 / 7.06
6.66	2	d (2.2 Hz)	**105.16**	**100.31, 126.79, 141.35, 162.49**	6.77 / 7.38
6.77	2	d (8.6 Hz)	**116.49**	**126.79, 130.00, 158.53**	
6.90	1	d (16.3 Hz)	**126.79 (130.00)**	**105.16, 130.00, 128.94, 141.35**	
7.06	1	d (16.3 Hz)	**130.00 (126.79)**	**105.16, 126.79, 128.94, 141.35**	
7.38	2	d (8.5 Hz)	**128.94**	**116.49, 130.00, 158.53**	
			130.29		
			141.35		
			158.53		
			162.49		
			155.49		
			161.06		

Table 23 ^{1}H and ^{13}C NMR spectral data of PS-B

PS-B (Santal)					
δ H [ppm]	Protonen - anzahl	Multiplizität (J in Hz)	δ C [ppm]	δ C [ppm] aus HMBC	COSY
3.88	3	s	**56.46**	**167.29**	6.36 / 6.53
6.36	1	d (2.3)	**99.24**	**93.21, 107.12, 163.65, 167.29**	6.85 / 7.03
6.53	1	d (2.3)	**93.21**	**99.24, 107.12, 159.57, 167.29**	
6.84	2	dd (14.6, 5.1)	**116.32**	**117.4, 123.64, 125.07, 146.27**	
			121.65	**117.4, 125.07, 146.90**	
7.03	1	d (2.0)	**117.40**	**121.65, 125.07, 146.27, 146.9**	
8.09	1	s	**155.10**	**123.64, 125.07, 159.57, 182.4**	
			107.12		
			123.64		
			125.07		
			146.27		
			146.90		
			159.57		
			163.65		
			167.29		
			182.40		

6.2 Phenotypic Screening of Selected Samples Affecting the Lifespan of *Caenorhabditis elegans*

6.2.1 Lifespan Assay

The exact procedure of the life span assay is described in the methods part of the diploma thesis by former students Anna Thrakl and Kevin Mészáros. Briefly, synchronized adult worms were assayed for lifespan prolonging effects in a *C. elegans* lifespan assay, using DMSO 1% as vehicle control and reserpine 30 µM as positive control. All living and dead worms were counted two to three times per week and the survival population was noted until more than 50% of the population was dead (DT_{50}).

6.2.2 Juglone-induced Stress Resistance Assay

The pro-oxidative compound juglone is commonly used to determine *C. elegans* vulnerability towards oxidative stress (Naß, Abdelfatah, & Efferth, 2021). Similar as in the lifespan assay, 5 – 15 synchronized adult worms are pre-treated for five days at 25 °C with the respective compounds before adding 80 µM (f.c.) juglone to the worm culture. 48 h after juglone treatment the survival of the nematodes is monitored.

6.3 Instruments, Solvents and Reagents

6.3.1 Instruments

Device	Technical Features / Description
Analytical Balance	Sartorius BP210D
Balance	Sartorius LC4801P
Concentrator	Sample Concentrator FSC400D, Techne
Hot Air Dryer	HG 2000 E, Steinel
HPCCC	Spectrum Dynamic extractions
Flash Chromatography	Interchim puriFlash 4250 Software: Interchim soft
Incubator	Memmert GTR0214
Incubator	Haereus
Microscope	Nikon Labophot-2; Reichert-Jung Neovar 2
NMR	Bruker NMR 500 MHz with cryo probe
Rotavary Evaporator	R-210, Büchi Laboratorium Technologie AG
Sephadex	Sephadex LH-20
TLC Spray Cabinet	CAMAG TLC spray cabinet II
TLC Visualizer	CAMAG
Ultrasonic Bath	Transsonic T 460, Elma
UPLC	Waters Acquity UPLC H-Class Modules: PDA, ELSD, ISM and QDa; Software: Empower
UV Lamp	CAMAG
Vacuum Pump	V-710, Büchi
Vortex mixer	Genius 3, IKA
Waterbath	Wasserbad GFL 1023

6.3.2 Solvents and Reagents

Solvents and Reagents	Description
Acetonitrile	HiPerSolv CHROMANORM® ≥99.9%, gradient grade for HPLC
Acetic Acid	Acidum aceticum conc., Gatt-Koller
Dichlormethane	Rectapur (distilled according to ÖAB)
Ethanol 96%	ÖAB distilled
Ethyl acetate	ÖAB distilled
Formic Acid 99%	≥ 98%, p.a., ACS, Carl Roth GmbH
Methanol	ÖAB distilled
Methanol	HiPerSolv CHROMANORM® ≥99.8%, for HPLC
n-Hexane	ÖAB distilled
Petroleum ether	ÖAB distilled
Water	Double distilled

6.3.3 Thin-Layer Chromatography

6.3.3.1 Spraying Reagents

Spraying reagent: Sulfuric Acid – Vanillin;

Sulfuric Acid, 5% in Methanol; Vanillin 1% in Methanol

6.3.3.2 TLC Plates

Merck TLC Silica Gel 60 F_{254} 20 x 20 cm

6.3.4 UPLC-Column

Waters ACQUITY UPLC® HSS T3 1.8 µm, 2,1 x 100mm Column, S/No: 01643501416082

7 REFERENCES

Websites

Images

https://commons.wikimedia.org/wiki/File:Red_sanders_tree,bramamgarimattam,A.P_-_panoramio.jpg, effective: May 2021

https://propropertiesindia.com/wp-content/uploads/2021/03/SANDALWOOD.jpg, effective: May 2021

Papers

Arunakumara, K., Walpola, B., Subasinghe, S., & Yoon, M. (2011). Pterocarpus santalinus Linn. f. (Rath handun): A Review of Its Botany, Uses, Phytochemistry and Pharmacology. *J. Korean Soc. Appl. Biol. Chem. 54(4)*, 495-500.

Arunkumar, A., & Joshi, G. (2014). Pterocarpus santalinus (Red Sanders) an Endemic, Endangered Tree of India: Current Status, Improvement and the Future. *Journal of Tropical Forestry and Environment Vol. 4(2)*, 1-10.

Back, P., Braeckman, B. P., & Matthijssens, F. (2012). ROS in Aging Caenorhabditis elegans: Damage or Signaling? *Oxidative Medicine and Cellular Longevity*, 1-14.

Biswas, T. K., Maity, L. N., & Mukhherjee, B. (2004). Wound healing potential of Pterocarpus santalinus linn: a pharmacological evaluation. *Int J Low Extrem Wounds 3(3)*, 143-150.

Blackwell, T. K., Steinbaugh, M. J., Hourihan, J. M., Ewald, C. Y., & Isik, M. (2015). SKN-1/Nrf, stress responses, and aging in Caenorhabditis elegans. *Free Radic Biol Med. 88*, 290-301.

Carmona, J. J., & Michan, S. (2016). Biology of healthy aging and longevity. *Rev. ives. clin. 68*, 7-16.

Cho, J., Park, J., Kim, P. S., Yoo, E. S., Baik, K. U., & Park, M. H. (2001). Savinin, a Lignan from Pterocarpus santalinus Inhibits Tumor Necrosis Factor-α Production and T Cell Proliferation. *Biol. Pharm. Bull. 24(2)*, 167-171.

Halim, E., & Misra, A. (2011). The effects of the aqueous extract of Pterocarpus santalinus heartwood and vitamin E supplementation in streptozotocin-induced diabetic rats. *Journal of Medicinal Plants Research 5(3)*, 398-409.

Jung, K., Jeon, J.-S., Ahn, M.-J., Kim, C. Y., & Kim, J. (2012). Preparative Isolation and Purification of Flavonoids from Pterocarpus Santalinus using Centrifugal Partition Chromatography. *Journal of Liquid Chromatography & Related Technologies 35:17*, 2462-2470.

Kameswara Rao, B., Giri, R., Kesavulu, M. M., & Apparao, C. (2001). Effect of oral administration of bark extracts of Pterocarpus santalinus L. on blood glucose level in experimental animals . *Journal of Ethnopharmacology 74*, 69-74.

Kesari, A. N., Gupta, R. K., & Watal, G. (2004). Two aurone glycosides from heartwood of Pterocarpus santalinus. *Phytochemistry 65*, 3125-3129.

Kondeti, V. K., Badri, K. R., Maddirala, D. R., Thur, S., Fatima, S. S., Kasetti, R. B., & Rao, C. A. (2010). Effect of Pterocarpus santalinus bark, on blood glucose, serum lipids, plasma insulin and hepatic carbohydrate metabolic enzymes in streptozotocin-induced diabetic rats. *Food and Chemical Toxicology 48*, 1281-1287.

Krishnaswamy, N., & Sundaresan, C. (2012). Fascinating Organic Molecules from Nature 1. Some Exotic Red Pigments of Plant Origin. *RESONANCE*, 928-932.

Krishnaveni, K. S., & Srinivasa Rao, J. V. (2000). A new isoflavone glucoside from Pterocarpus santalinus. *J Asian Nat Prod Res 2(3)*, 219-223.

Kumar, D. (2011). Anti-inflammatory, analgesic, and antioxidant activities of methanolic wood extract of Pterocarpus santalinus L. *Journal of Pharmacology & Pharmacotherapeutics 2(3)*, 200-202.

Kumar, N., Ravindranath, B., & Seshadri, T. R. (1974). Terpenoids of Pterocarpus Santalinus Heartwood. *Phytochemistry Vol. 13*, 633-636.

Kwon, H. J., Hong, Y. K., Kim, K. H., Han, C. H., Cho, S. H., Choi, J. S., & Kim, B.-W. (2006). Methanolic extract of Pterocarpus santalinus induces apoptosis in HeLa cells. *Journal of Ethnophharmacology 105*, 229-234.

Li, L., Tao, R.-H., Wu, J.-M., Guo, Y.-P., Huang, C., Liang, H.-G., . . . Wang, J.-H. (2018). Three new sesquiterpenes from Pterocarpus santalinus. *Journal of Asian Natural Products Research 20(4)*, 306-312.

Li, Y.-R., Li, S., & Lin, C.-C. (2018). Effect of resveratrol and pterostilbene on aging and longevity. *Biofactors 44 (1)*, 69-82.

Manjunatha, B. K. (2006). Antibacterial Activity of Pterocarpus santalinus. *Indian Journal of Pharmaceutical Sciences 68(1)*, 115-116.

Manjunatha, B. K. (2006). Hepatoprotective activity of Pterocarpus santalinus L.f.,an endangered medicinal plant 38. *Indian Journal of Pharmacology*, 25-28.

Martins, R., Lithgow, G. J., & Link, W. (2016). Long live FOXO: unraveling the role of FOXO proteins in aging and longevity. *Aging Cell 15*, 196-207.

Mishra, M. P., & Padhy, R. N. (2013). In Vitro Antibacterial Efficacy of 21 Indian Timber-Yielding Plants Against Multidrug- Resistant Bacteria Causing Urinary Tract Infection. *Osong Public Health Res Perspect 4(6)*, 347-357.

Mohammad, A., Rajkapoor, B., & Kavimani, S. (2015). A REVIEW ON PTEROCARPUS SANTALINUS LINN. *World Journal of pharmaceutical Research Vol. 4(2)*, 282-292.

Naß, J., Abdelfatah, S., & Efferth, T. (2021). The triterpenoid ursolic acid ameliorates stress in Caenorhabditis elegans by affecting the depression-associated genes skn-1 and prdx2. *Phytomedicine International Journal of Phytotherapy and Phytopharmacology*, 1-10.

Narayan, S., Devi, R. S., Srinivasan, P., & Shyamala Devi, C. S. (2005). Pterocarpus santalinus: A Traditional HerbalDrug as a Protectant Against IbuprofenInduced Gastric Ulcers. *Phytotherapy Research 19*, 958-962.

Navada, K., & Vittal, R. (2014). Ethnomedicinal value of Pterocarpus santalinus (Linn. f.), a Fabaceae member. *Orient Pharm Exp Med 14*, 313-317.

Obrador, E., Salvador-Palmer, R., Jihad-Jebbar, A., Lopez-Blanch, R., Dellinger, T. H., Dellinger, R. W., & Estrela, J. M. (2021). Pterostilbene in Cancer Therapy. *Antioxidants 10 492*, 1-17.

Remsberg, C. M., Yanez, J. A., Ohgami, Y., Vega-Villa, K. R., Rimando, A. M., & Davies, N. M. (2008). Pharmacometrics of Pterostilbene: Preclinical Pharmacokinetics and Metabolism, Anticancer, Antiinflammatory, Antioxidant and Analgesic Activity. *Phytotherapy Research 22*, 169-179.

Roge, A., Firke, S., Kawade, R., Sarje, S., & Vadvalkar, S. (2011, July). BRIEF REVIEW ON: FLASH CHROMATOGRAPHY. *International Journal of Pharmaceutical Scienes and Research, Issue 8*(2), Page 1930-1937.

Saradamma, B., Hymavathi, R., Varadacharyulu, N., & Damodara, R. V. (2016). Therapeutic Potential of Pterocarpus santalinus L.: An Update. *Pharmacognosy Rev. 10(19)*, 43-49.

Shen, P., Yue, Y., & Park, Y. (2018). A living model for obesity and aging research: Caenorhabditis elegans . *Critical Reviews in Food Science and Nutrition 58:5*, 741-754.

Soundararajan, V., Ravi Kumar, G., Murugesan, K., & Chandrashekar, B. S. (2016). A REVIEW ON RED SANDERS (PTEROCARPUS SANTALINUS LINN.) – PHYTO-CHEMISTRY AND PHARMACOLOGICAL IMPORTANCE . *World Journal of Pharmacy and pharmaceutical Sciences 5(6)*, 667-689.

Strych , S., Journot, G., Pemberton, R., Wang, S., Tantillo, D., & Trauner, D. (2015). Biomimetic Total Synthesis of Santalin Y. *Angewandte Chemie Int. Ed.*, 5079-5083.

Strych, S., & Trauner, D. (2013). Biomimetische Synthese von Santalin A,B und Santarubin A,B, den Hautpigmenten des Roten Sandelholzes. *Angew. Chem. 125*, 9687-9690.

Strych, S., & Trauner, D. (2013). Biomimetische Synthese von Santalin A,B und Santarubin A,B, den Hautpigmenten des Roten Sandelholzes. *Angewandte Chemie 125*, 9687-9690.

Thrakl, A. (2019). Unravelling the lifespan increasing potential of Pterocarpus santalinus in a phenotypic Caenorhabditis elegans lifespan assay. Universität Wien.

Torgovnick, A., Schiavi, A., Maglioni, S., & Ventura, N. (2013). Healthy aging: what can we learn from Caenorhabditis elegans? *Z Gerontol Geriat 46*, 623-628.

Vatner, S. F., Zhang, J., Oydanich, M., Berkman, T., Naftalovich, R., & Vatner, D. E. (2020). Healthful aging mediated by inhibition of oxidative stress. *Ageing Research Reviews 64*, 101194.

Wilson, M. A., Rimando, A. M., & Wolkow, C. A. (2008). Methoxylation enhances stilbene bioactivity in Caenorhabditis elegans. *BMC Pharmacology 8:15*, 1-11.

Wu, S.-F., Chang, F.-R., Wang, S.-Y., Hwang, T.-L., Lee, C.-L., Chen, S.-L., . . . Wu, Y.-C. (2011). Anti-inflammatory and Cytotoxic Neoflavonoids and Benzofurans from Pterocarpus santalinus. *Journal of Natural Products 74*, 989-996.

Wu, S.-F., Hwang, T.-L., Chen, S.-L., Wu, C.-C., Ohkoshi, E., Lee, K.-H., . . . Wu, Y.-C. (2011). Bioactive components from the heartwood of Pterocarpus santalinus. *Bioorganic & Medicinal Chemistry Letters 21*, 5630-5632.

Zhang, H., Davies, K., & Forman, H. J. (2015). Oxidative stress response and Nrf2 signaling in aging. *Free Radic Biol Med. 88(0 0)*, 314-336.

Zhang, Z. D., Milman, S., Lin, J.-R., Wierbowski, S., Yu, H., Barzilai, N., . . . Vijg, J. (2020). Genetics of extreme human longevity to guide drug discovery for healthy ageing. *Nat Metab. 2(8)*, 663-672.

Zwirchmayr, J., Kirchweger, B., Lehner, T., Tahir, A., Pretsch, D., & Rollinger, J. M. (2020). A robust and miniaturized screening platform to study natural products affecting metabolism and survival in Caenorhabditis elegans. *Sci Rep 10*.

8 APPENDIX

8.1 NMR Spectra

8.1.1 PS-A

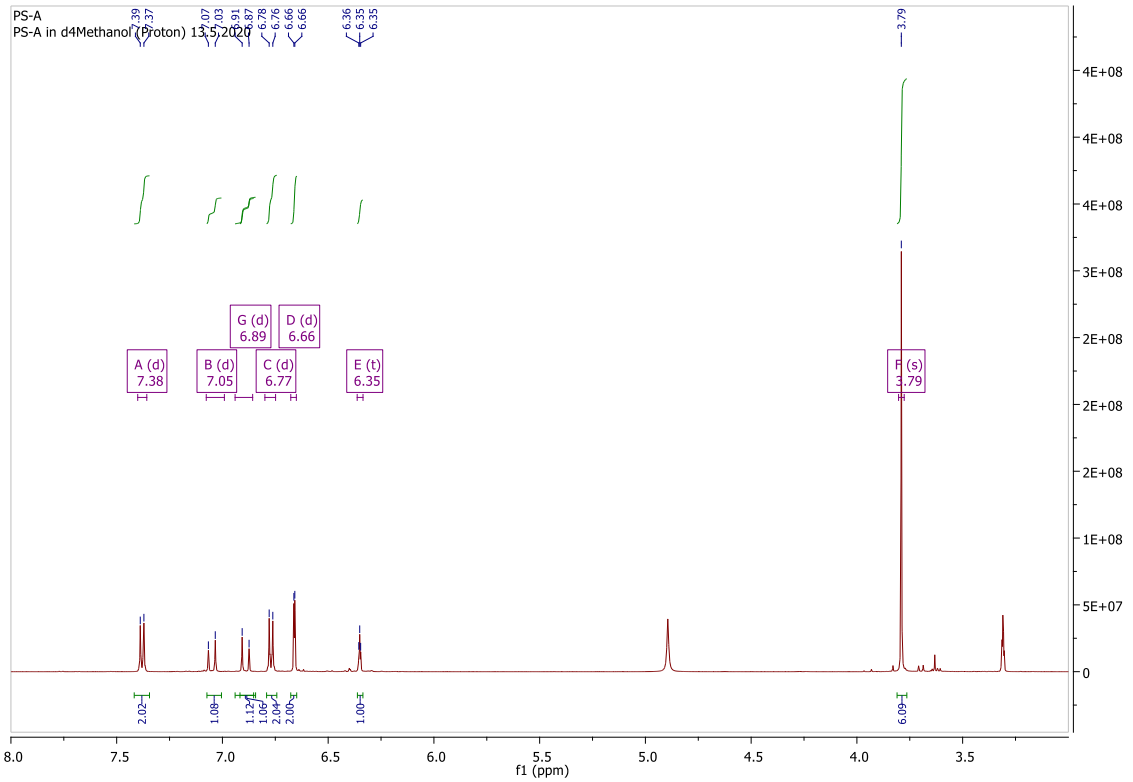

Figure 30: ^{1}H NMR spectrum of PS-A (MeOD, ref.: δH 3.31 ppm, 500 MHz NMR, ~1 mg)

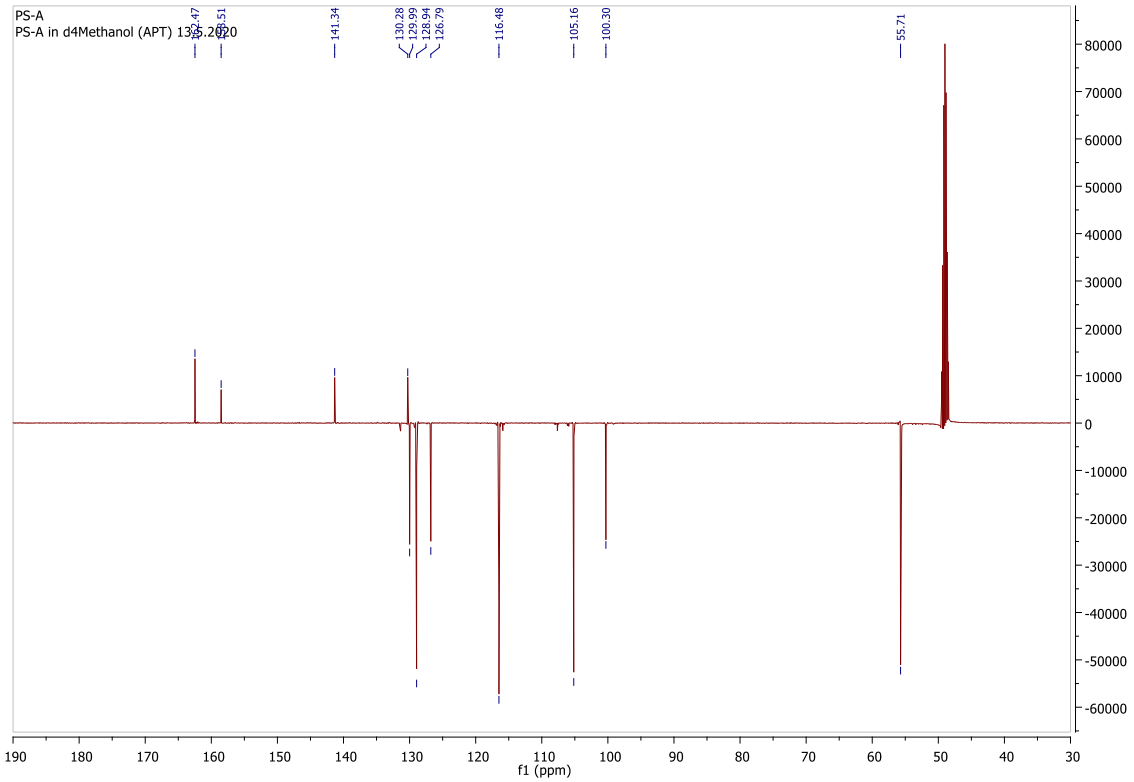

Figure 31: ^{13}C-APT NMR spectrum of PS-A (MeOD, ref.: δC 49.00 ppm, 500 MHz NMR, ~1 mg)

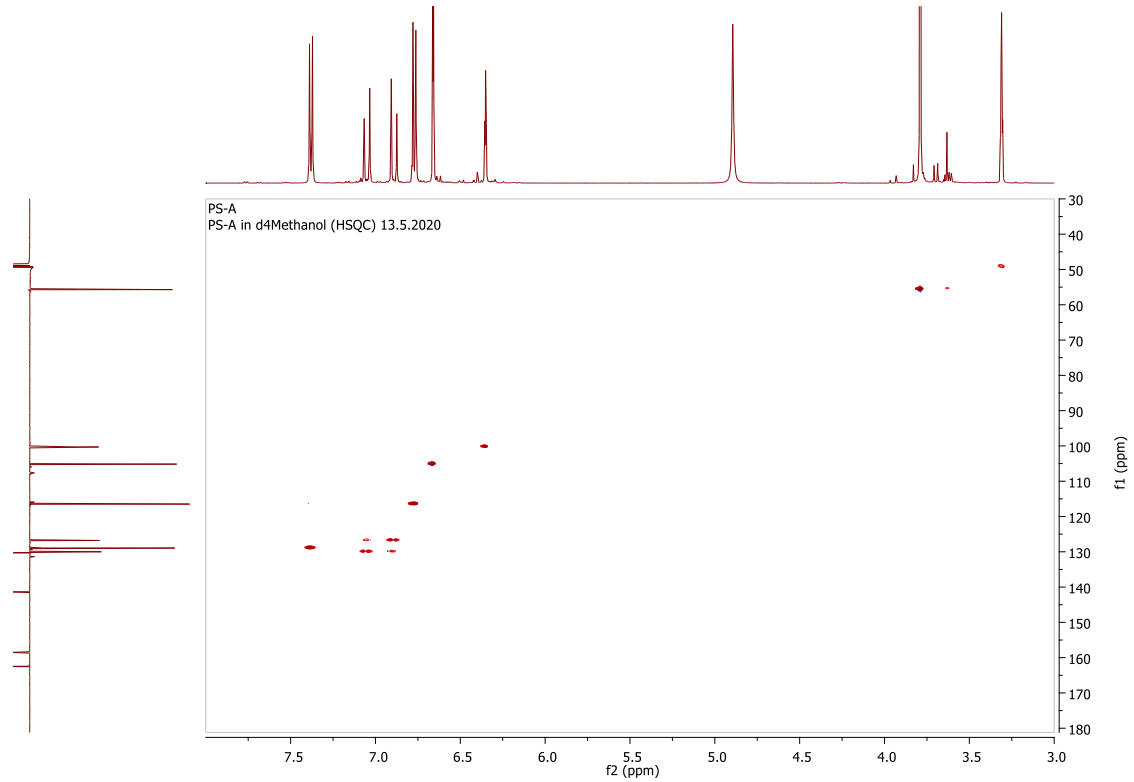

Figure 32: HSQC spectrum of PS-A (horizontal trace: ^{1}H NMR spectrum, vertical trace: 13C APT; MeOD, ref.: δH 3.31 ppm, δC 49.00 ppm, 500 MHz NMR, ~1 mg)

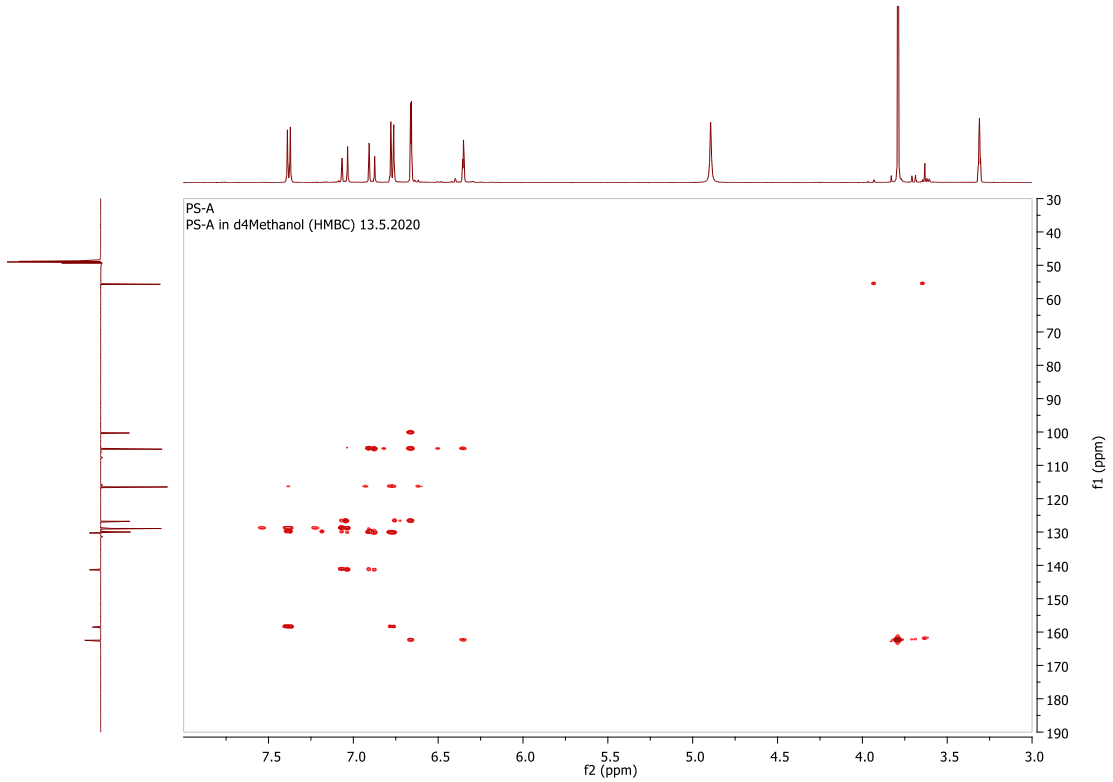

Figure 33: HMBC spectrum of PS-A (horizontal trace: ^{1}H NMR spectrum, vertical trace: 13C APT; MeOD, ref.: δH 3.31 ppm, δC 49.00 ppm, 500 MHz NMR, ~1 mg)

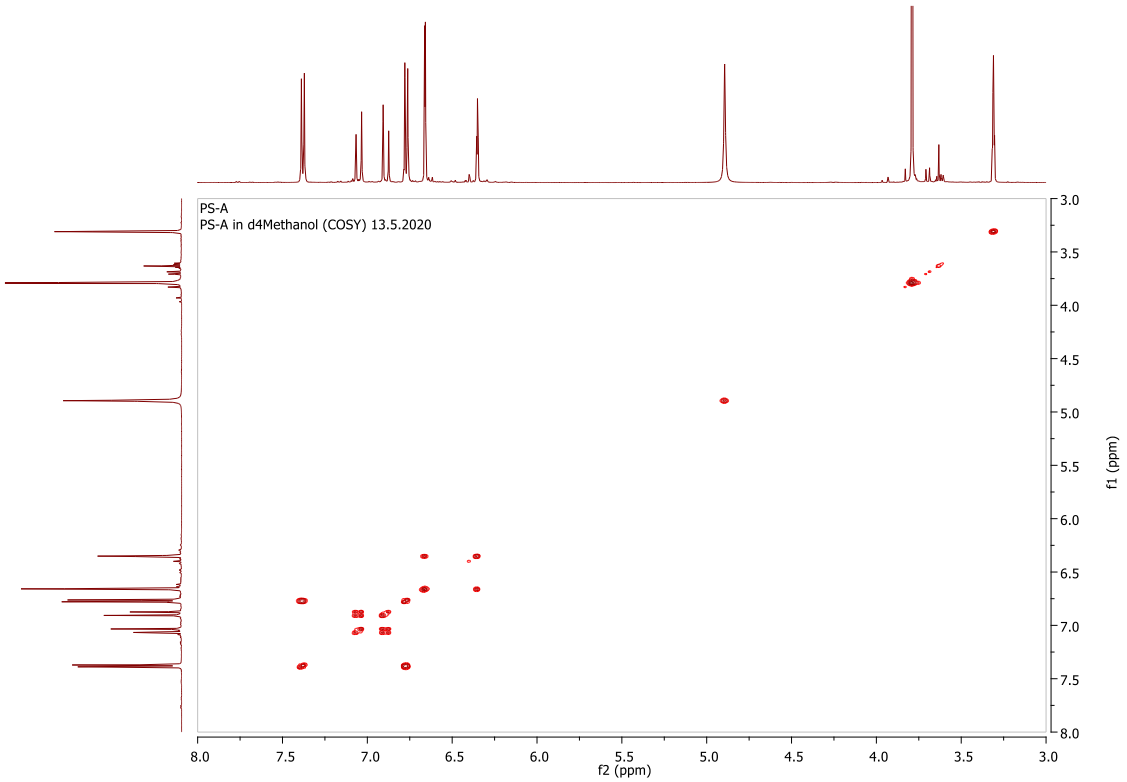

Figure 34: HH-COSY spectrum of PS-A (horizontal & vertical trace: 1H NMR spectrum; MeOD, ref.: δH 3.31 ppm, 500 MHz NMR, ~1 mg)

8.1.2 PS-B

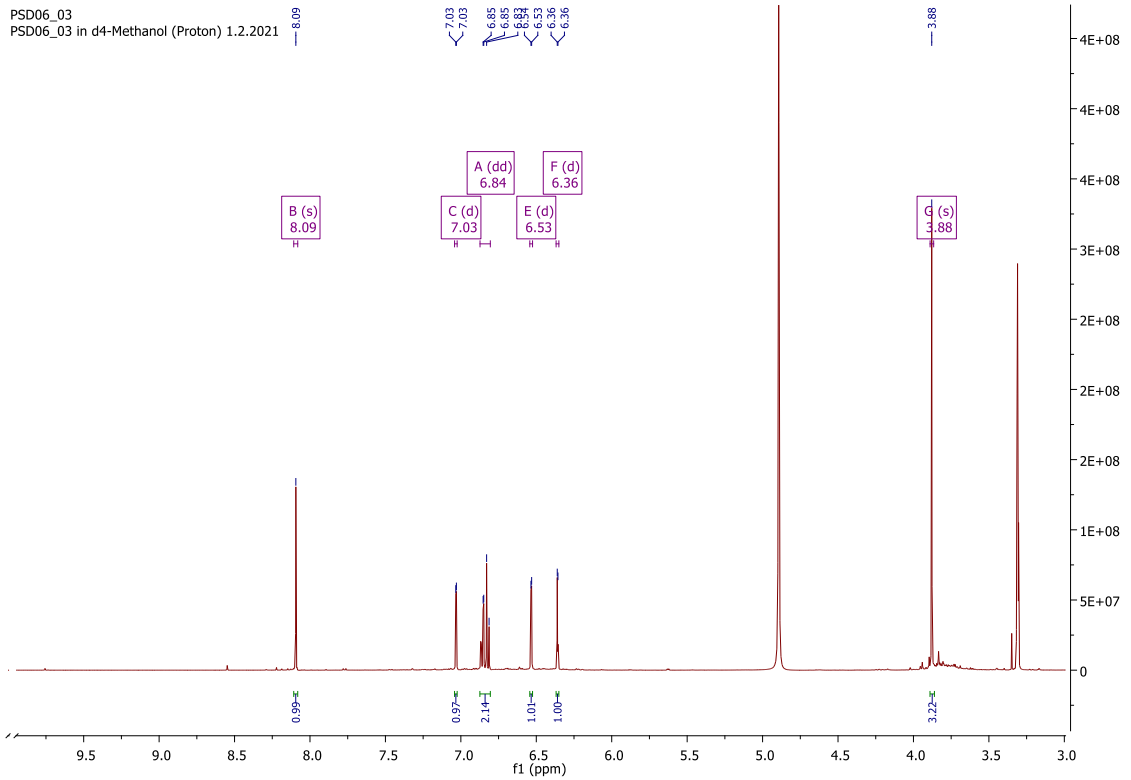

Figure 35: ^{1}H NMR spectrum of PS-B (MeOD, ref.: δH 3.31 ppm, 500 MHz NMR, ~1 mg)

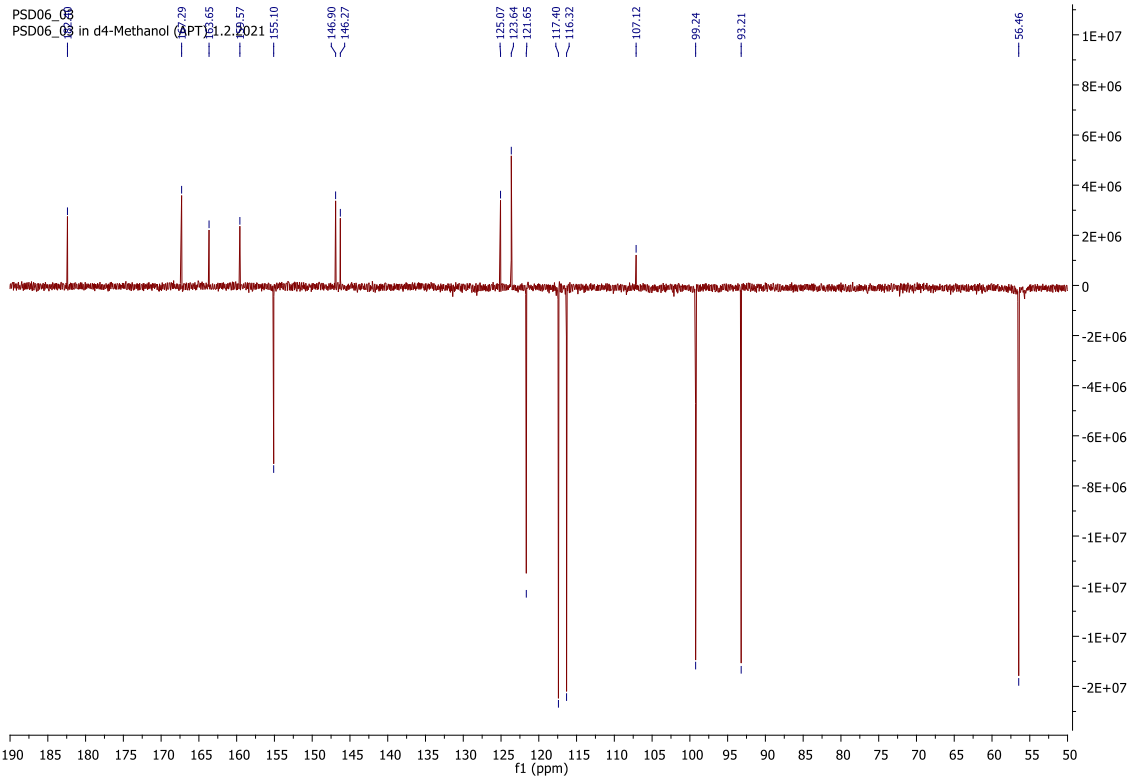

Figure 36: ^{13}C-APT NMR spectrum of PS-B (MeOD, ref.: δC 49.00 ppm, 500 MHz NMR, ~1 mg)

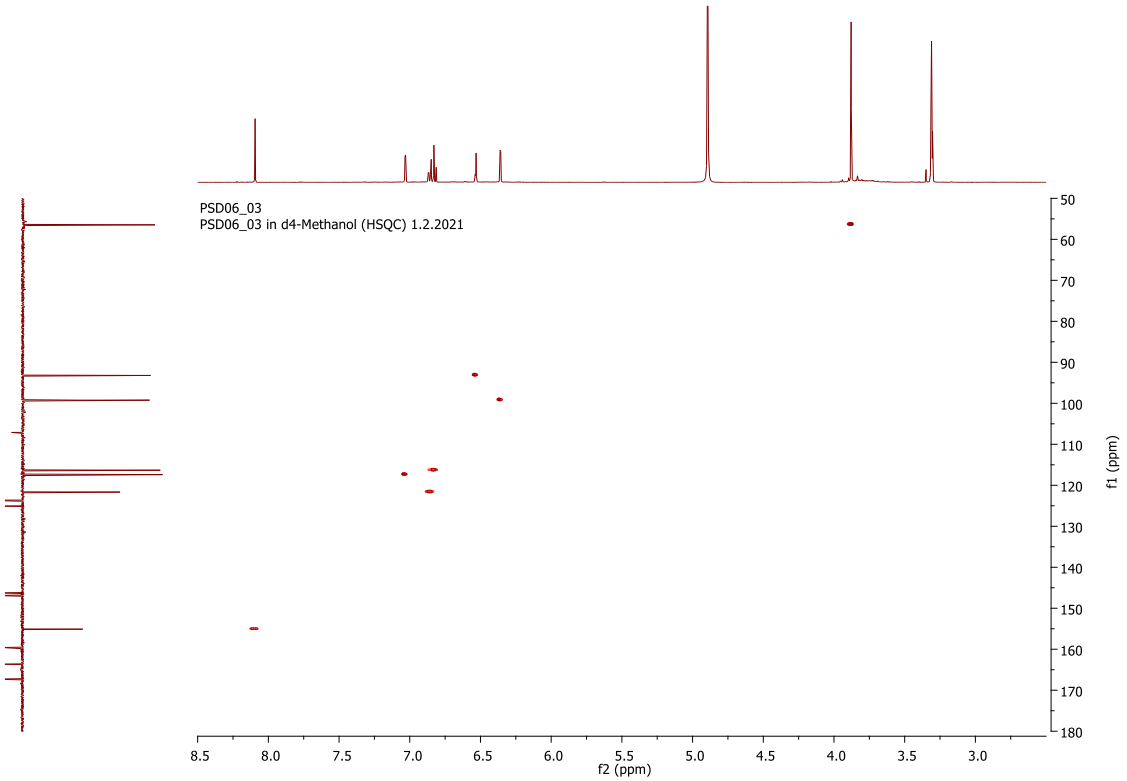

Figure 37: HSQC spectrum of PS-B (horizontal trace: ^{1}H NMR spectrum, vertical trace: ^{13}C APT; MeOD, ref.: δH 3.31 ppm, δC 49.00 ppm, 500 MHz NMR, ~1 mg)

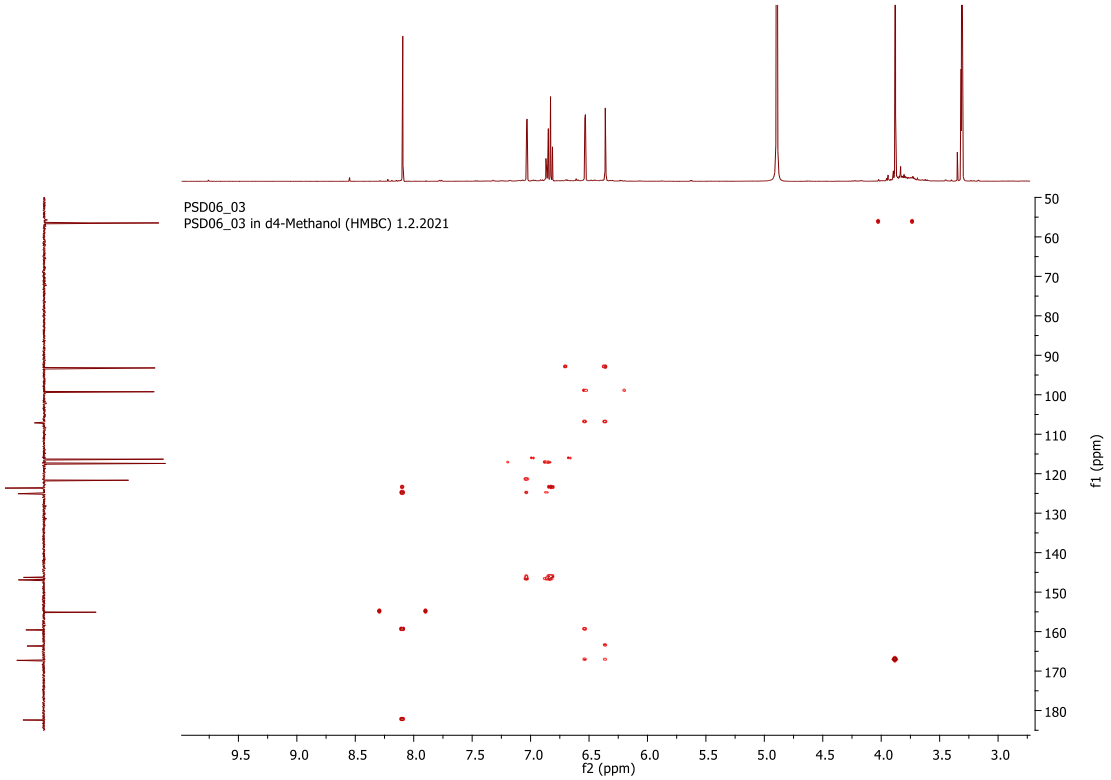

Figure 38: HMBC spectrum of PS-B (horizontal trace: ^{1}H NMR spectrum, vertical trace: ^{13}C APT; MeOD, ref.: δH 3.31 ppm, δC 49.00 ppm, 500 MHz NMR, ~1 mg)

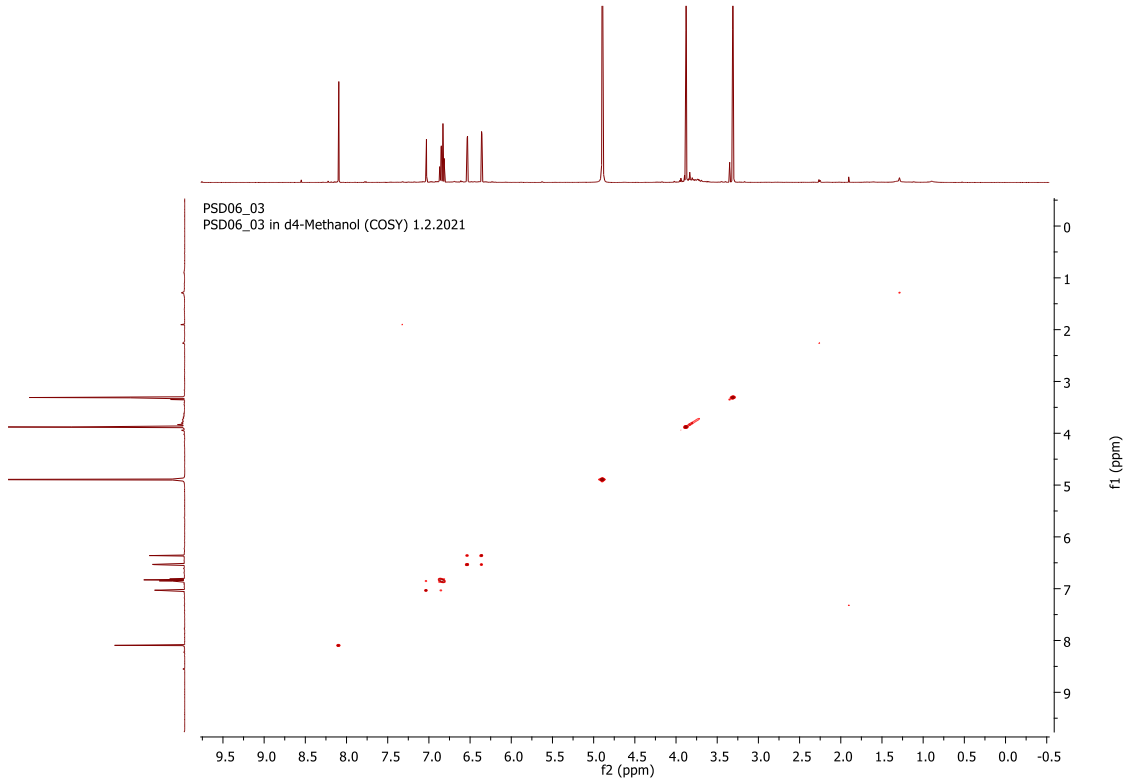

Figure 39: HH-COSY spectrum of PS-B (horizontal & vertical trace: ^{1}H NMR spectrum; MeOD, ref.: δH 3.31 ppm, 500 MHz NMR, ~1 mg)